Erectile Dysfunction and Penile Skin Temperature

The Possibility of Continuous Penile Skin Temperature Measurements to Monitor Sleep-Related Erections

Roos Edgar

October 15, 2021

Graduation committee

St. Antonius Hospital

Dr. J.J.H. Beck MD, medical supervisor

University of Twente

Prof.dr.ir. P.H. Veltink, committee chair

Dr.ir. W. Olthuis, technical supervisor

Dr. M. Groenier, process supervisor

Dr. A.T.M. Bellos-Grob, external committee member

ZIEKENHUIS ST ANTONIUS

UNIVERSITY OF TWENTE.

Abstract

INTRODUCTION - Erectile Dysfunction (ED) is a frequently occurring disorder and affects the quality of life and sexual satisfaction of numerous men. The golden standard for diagnosing the either somatic or psychogenic cause of ED is by monitoring Sleep-Related Erections (SREs) by the RigiScan. This outdated sensing system has several drawbacks and needs replacement. In a previous study, we introduced several alternative methods for the monitoring of SREs, including the possibility of penile skin temperature monitoring. The objective of this study is to find out whether penile skin temperature measurements are suitable for the monitoring of SREs.

HEAT TRANSFER MODEL - A mathematical model is set up to describe the thermal aspects that occur during a flaccid state and an erection. The heat transfer is described by means of conduction and convection in a closed system model with steady state, steady flow condition. Parameters and constants are found in literature or determined experimentally. According to our model, the temperature increase from flaccid to erect state is 1.4 °C, in naked condition. When wearing clothes (i.e. cotton underwear) and clothes plus a blanket, we calculated a temperature increase of 1.1 °C and 0.4 °C respectively.

METHODS - Nighttime penile skin temperature monitoring is carried out in one healthy subject (age 28) with the TM-220 thermistor (iWorx Systems inc, Dover, USA), and compared to the outcomes of the RigiScan (GOTOP Medical Inc., St. Paul, Minnesota, USA). Low- and high-pass filters are applied to the temperature data to remove high-frequency noise and the circadian cycle. Next, time and temperature intervals are extracted that correspond to erections in the RigiScan data. These intervals are used for slope analysis. Wilcoxon signed-rank tests are applied to test for significant differences in the non-normal distributed data.

RESULTS - In total, 22 erections are monitored during 7 nights. The penile skin temperature varies between 32 °C and 36 °C. The mean duration of the erections is 25.4 minutes (SD 12.8). The Wilcoxon signed-rank test reveals that the temperature at t = 10 minutes in every erection interval is significantly higher than the temperature at t = 0 minutes ($p = 0.009$). The temperature slopes of intervals where erections take place are not significantly different compared to the slopes of the non-erection intervals (complete interval; $p = 0.306$, first 10 minutes of each interval; $p = 0.123$).

DISCUSSION AND CONCLUSION - Despite the promising results from our heat transfer model, we cannot distinguish an erection from a non-erection in one healthy subject by measuring skin temperature yet. The statistical proof of a temperature rise during an erection is poor, but we do see some changes. Unfortunately, the interquartile ranges exceed the medians. Probably, ambient temperature fluctuations resulted in too much disturbance which influenced the data obtained. Therefore, further research should focus on minimizing those fluctuations in the temperature measurements. All in all, the importance of our results lies both in pioneering in this field and the search towards a worthy successor of the RigiScan in general.

Keywords - Erectile Dysfunction, Sleep-Related Erections, Heat transfer, Thermistor, RigiScan

Contents

Abbreviations and symbols

Abbreviations

ED	Erectile Dysfunction
H_0	Null hypothesis
IIEF-5	Five-item International Index of Erectile Dysfunction
IQR	Interquartile Range
NO	Nitric Oxide
NTC	Negative Temperature Coefficient
REM	Rapid Eye Movement
SD	Standard Deviation
SRE	Sleep-Related Erection

Symbols and units

ΔT	Temperature difference $[K]$
$\dot{Q}$	Heat flow $[W]$
$\dot{q}$	Heat generation per unit volume $[W/m^3]$
$\dot{Q}_{cond}$	Conductive heat flow $[W]$
$\dot{Q}_{conv}$	Convective heat flow $[W]$
ρ	Density $[kg/m^3]$
A	Area $[m^2]$
C, C_1, C_2	Constants of integration [-]
c_p	Specific heat $[J/kgK]$
h	Convective heat transfer coefficient $[W/m^2K]$
k	Thermal conductivity $[J/msK]$ or $[W/mK]$
k_f	Thermal conductivity of the fluid $[J/msK]$ or $[W/mK]$
L	Penile length $[m]$
m	Mass $[kg]$
q''	Heat flux per unit area $[W/m^2]$
q''_s	Heat flux per unit area at the surface $[W/m^2]$
r	Radius $[m]$
r, φ, z	Cylindrical coordinates; radius, angle and height [-]
r_1	Inner radius $[m]$
r_2	Outer radius $[m]$
R_{cond}	Conductive thermal resistance $[K/W]$
R_{conv}	Convective thermal resistance $[K/W]$
r_{conv}	Convection radius $[m]$
R_{tot}	Total thermal resistance $[K/W]$

T	Temperature $[K]$
t	Time $[s]$
T_1	Temperature at r_1 $[K]$
T_2	Temperature at r_2 $[K]$
T_i	Initial temperature $[K]$
T_s	Skin temperature $[K]$
T_∞	Temperature of the environment $[K]$
T_{blood}	Temperature of the blood $[K]$
V	Volume $[m^3]$
x	Distance in the direction of the heat flow $[m]$

1 Introduction

Most men associate their manhood with a well-functioning penis [1]. Therefore, it is not surprising that a loss of erectile function seriously affects the quality of life and sexual satisfaction [2]. ED, defined as the inability to attain and/or maintain penile erection sufficient for satisfactory sexual performance [3], is a frequently occurring disorder. The prevalence of ED varies widely, possibly due to different definitions of ED or differences in information collection [4]. The review of Lewis et al.[4] (2010) describes a prevalence of 1-10% for the population <40 years, from 2-9% up to 15% for ages between 40-49 years, a great variety for 50-59 years, 20-40% for the ages 60-69 years, and a very high prevalence of 50-100% among men in their 70s and 80s. There are several underlying causes of this complex health problem, which can be divided into somatic (or physiological) causes, psychogenic (or psychological) causes, and a combination of the two [5]. Increasing age plays a major role in the risk of developing ED as well, as the disorder mainly affects men older than 40 years [4, 5, 6]. It has been estimated that approximately 322 million men worldwide will suffer from ED by the time of 2025, taking into account the increasingly aging population [6].

The severity of ED can be characterized with the help of the five-item International Index of Erectile Function (IIEF-5) questionnaire, ranging from none (score 22–25) to severe ED (score 1-7) [7]. For a classification between a somatic or psychogenic cause of ED, home monitoring of SREs with the RigiScan is the golden standard [8]. This sensing system is dating from 1985 and has several drawbacks. Furthermore, it is not possible to replace any of the parts since they stopped delivering orders to the Netherlands. A detailed description of the RigiScan can be found in our earlier study [9] (see Appendix A). Diagnosing ED is not only important for the right therapy but may have an impact on the general health as well. For example, a meta-analysis of Dong et al. [10] (2011) showed that ED is a precursor of cardiovascular disease. Moreover, they suggest that ED significantly increases the risk of stroke, coronary heart disease, and all-cause mortality [10]. Therefore, an adequate diagnostic method is essential. Still, state-of-the-art diagnostic techniques are lacking. In our study, we are working towards a new method for diagnosing ED. Several studies underline the importance of the development of a new diagnostic method for ED [6, 9, 11, 12]. This is also confirmed in a survey study conducted by St. Antonius hospital Nieuwegein. The survey was filled in by 87 Dutch health care professionals who see patients with ED on a regular. One question was devoted to evaluate the opinion of the respondents on the most important requirements of a new device. In Figure 1, an overview of the outcome of this question is given.

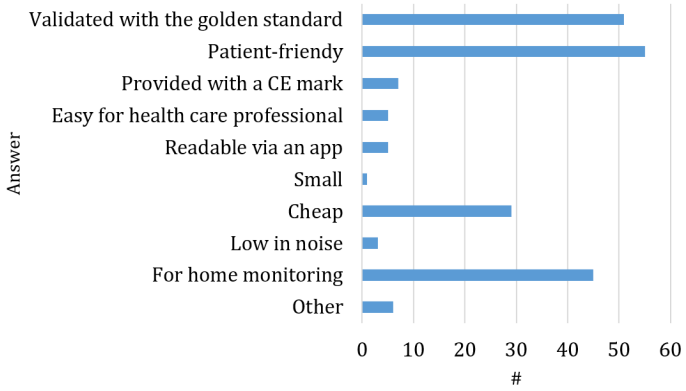

Figure 1: *The most important sensor requirements for a new sensing system, according to 87 health care professionals. Every respondent chose three answers. The requirement that was selected the most is patient-friendly.*

In our previous study, we introduced penile skin temperature measurements as a potential method to monitor SREs [9] (see Appendix A). Various studies found an increase in penile skin temperature during sexual arousal due to the accumulation of blood in the corpora cavernosa [13, 14, 15, 16, 17, 18]. For the evaluation of penile temperature changes, most of these studies used thermography and a few used a thermistor for direct skin temperature measurements. Nevertheless, the findings were similar. Kukkonen performed two studies among healthy individuals and found an average penile skin temperature increase during an erection of 2.6°C among men of 18-29 years old [15] and an increase of

1.2°C in the age group of 30-45 years old [16]. In the current study, we further investigate the use of a temperature sensor for the monitoring of penile erections.

1.1 Aim of the study

The objective of this study is to find out whether penile skin temperature measurements are suitable for the monitoring of SREs. We approach this problem in different ways. First, the thermodynamic aspects of the penis are described in a heat transfer model. The influence of an alternating environment temperature is taken into account as well. Thereafter, penile skin temperature measurements as a method for the monitoring of SREs are compared to the golden standard (i.e. RigiScan) in a healthy subject. It is hypothesized that a temperature sensor measures an increase in penile skin temperature during an erection and a decrease in temperature afterwards. The different parts of this study lead to new insights and future recommendations. Afterwards, we can answer the following research question and sub-questions:

Is it possible to monitor sleep-related erections at home with the help of continuous penile skin temperature measurements?

1. How can we describe the thermal aspects of the penile heat transfer during a flaccid condition and an erection?
2. What is the influence of blankets and clothes on continuous (penile) skin temperature measurements?
3. What is the correlation between SREs monitored by the golden standard and by a skin temperature sensor in healthy subjects?
4. What are the next steps towards a new sensing system for the monitoring of SREs?

2 Clinical background

2.1 Normal erectile function

The process of tumescence (= engorgement of erectile tissues) and detumescence (= subsiding from a state of swelling) can be divided into several phases. In the flaccid phase, the sympathetic nervous system dominates and the cavernous smooth muscles are contracted. The blood supply by the cavernous arteries (see Figure 2) is solely for nutritional purposes, and the venous outflow is unrestricted. During sexual arousal, the parasympathetic influence dominates the sympathetic nervous system. This leads to an increased blood flow and decreased peripheral resistance due to dilatation of the arterial blood vessels. The influx of blood increases rapidly. Relaxation of the cavernosal smooth muscles causes an increase in cavernosal compliance, which results in penile engorgement. During the full erection phase, the increased cavernosal pressure comes close to the systolic blood pressure which results in occlusion of venous outflow. This so-called veno-occlusive mechanism results in the rigid penile erection phase. In this phase, the cavernosal pressure exceeds the systolic blood pressure and the cavernous artery flow stagnates [19, 20, 21, 22].

Loss of penile erection is called detumescence and occurs when sexual arousal ends or after ejaculation. The sympathetic nervous system takes over again and the smooth muscles contract, which leads to a decrease in intracavernous pressure. With a decrease of compressive force, the venous outflow increases. The arterial flow returns to its normal rate [19, 21].

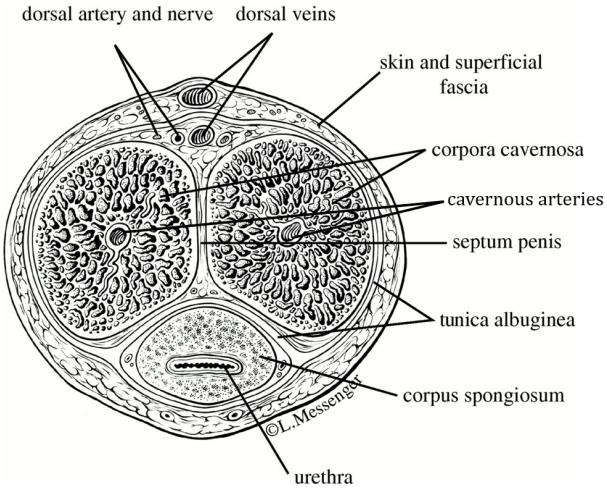

Figure 2: *A schematic view of the cross-section of the penis. The figure is modified from Udelson et al. [23].*

It is normal for healthy men to have three to six erections each night during rapid eye movement (REM) sleep, also referred to as SREs [24]. During REM sleep, pathways from the hypothalamus lead to increased parasympathetic neural activity and decreased sympathetic activity. Nitric oxide (NO), a neurotransmitter released from the parasympathetic nerves, leads to relaxation of the cavernosal smooth muscles. As a result, the trabecular spaces of the cavernosal bodies fill with blood and the venous outflow is reduced due to compression of the cavernosal veins against the tunica albuginea [22, 25]. At the end of REM sleep, detumescence takes place due to the dominating sympathetic nervous system. The intensity and duration of SREs decline with age [26].

2.2 Impaired erectile function

In general, ED has a somatic or psychogenic cause. The somatic causes can be classified as neurogenic, vasculogenic, drug-induced, endocrinological, and general lifestyle [2, 5]. *Neurological* disorders that may influence penile functioning include multiple sclerosis, spinal cord injury, Parkinson's disease, and strokes. Pelvic neuronal damage can also occur after prostatectomy. Additionally, diabetes and alcoholism affect dorsal nerve endings that can lead to ED [5]. *Vascular* problems leading to ED include endothelial dysfunction. Impaired blood flow may be caused by cardiovascular disease, cigarette smoking, diabetes, and hypertension [5, 27]. Examples of classes of *drugs* that may be associated with ED

include psychotropic (serotonin reuptake inhibitors, venlafaxine), anti-psychotic (rispiridone, olanzapine), and anti-hypertensive drugs [28, 29]. Moreover, excessive use of recreational drugs might influence erectile function [5]. *Endocrinological* causes of ED include a deficiency of male sex hormones (androgens), such as hormones responsible for testosterone secretion or NO synthesis [5]. Furthermore, *general lifestyle* has an impact on erectile functioning. As mentioned earlier, age is the primary risk factor for the development of ED [4]. Moreover, comorbidities such as diabetes mellitus type 2, obesity, and sleep disorders are associated with ED [4, 30]. A sedentary lifestyle, alcohol misuse, and smoking also play a role in developing ED [5, 31]. A form of somatic ED often involves a psychogenic response as well, since ED imposes negative effects on the quality of life and sexual relationships [2]. For example, when a men's erections become less rigid due to a somatic cause, this can be accompanied by insecurities. The psychological component of these insecurities may lead to a further decline in the quality of the erections, which provokes a vicious circle.

Common causes of psychogenic ED are depression, performance anxiety, stress, and anatomical variations [2, 5]. Furthermore, relationship problems and family or social pressures also affect erectile functioning [5]. Symptoms of a psychogenic ED include a sudden onset of dysfunction, intermittent function (situational), incapable of sustaining an erection, and normal SREs [2]. The anxiety that comes with psychogenic ED can lead to an increased focus on the quality of a man's erection. The latter results in self-consciousness and distractions that negatively impact sexual arousal, contributing to poor performance. As a result, the pressure to perform in the future rises which increases the likelihood of failure [2, 32].

3 Heat transfer model

Heat transfer from the core to the skin occurs through convection of blood from the arteries to the capillaries, and through passive conduction from the core via the tissues. Most of the generated heat leaves the core by convection. The proportionality of conduction is relatively fixed, because of a fixed thickness of insulation (subcutaneous fat). The proportionality of convection, on the other hand, is much more variable due to e.g. vasoconstriction and vasodilatation. Heat loss from the body surface to the environment occurs via radiation and convection [33]. In our model, we will focus on conduction and convection as heat transfer mechanisms. Since we are talking about an organ that is only a small portion of the total body and a temperature difference of approximately $2°C$, radiation plays a negligible role in the heat transfer. In this model, the law of conservation of energy is in effect, thus the energy is conserved over time [34]. An estimation of the total heat flow ($\dot{Q}\ [W]$) can be made by dividing the total temperature difference ($\Delta T\ [K]$) by the thermal resistance of the whole system ($R_{tot}\ [K/W]$) [34].

$$\dot{Q} = \frac{\Delta T}{R_{tot}} = \frac{T_{blood} - T_{\infty}}{R_{tot}} \tag{1}$$

The temperature of the blood ($T_{blood}\ [K]$) and the environment ($T_{\infty}\ [K]$) are known. The general equation for the total thermal resistance consists of a conductive and convective resistance which are in series, see equation (2).

$$R_{tot} = \frac{x}{kA} + \frac{1}{hA} \tag{2}$$

The convective heat transfer coefficient of the environment (h) and the thermal conductivity (k) are described later on. The area of the surface is described by $A\ [m^2]$. The distance in the direction of the heat flow is described by $x\ [m]$. Below in section 3.1, we start by defining the assumptions of our model. Thereafter, the contribution from conduction and convection to the heat transfer are described, in section 3.2 and 3.3 respectively. Although these processes take place simultaneously we discuss them in separate sections, after which they reunite in section 3.4. Here, we present the outcomes of our model.

3.1 Assumptions

Below, the assumptions of this model are listed.

- Energy can be exchanged with its surroundings, but not matter. Therefore, it is a closed system.
- There is a steady state, steady flow condition.
- Both corpora cavernosa are described as being one blood reservoir. The heat transfer is described from the inside of the corpus cavernosum towards the skin. The corpus spongiosum is not taken into account.
- There are two states: flaccid and erect.
- The penis is described as a cylinder in a bigger cylinder, with radius (r), angle (φ) and height (z), see Figure 3a. The inner cylinder is the blood compartment, or the corpora cavernosa. The outer cylinder is the connective tissue, including the skin and different fascias. Heat is transferred from the hotter inner cylinder via the outer cylinder towards the colder environment. Conductive heat transfer will be described in the r-direction. Therefore, heat flow in φ-direction and z-direction is considered to be zero.

To draw conclusions about the influence of the environmental temperature on the skin temperature measurements and the contact surface area of the sensor, two different situations will be described. See Figure 3b. Black dots indicate three different temperatures: (1) the temperature of the blood compartment, (2) the temperature of the skin surface, and (3) the temperature of the environment. Heat flows from 1 towards 3. During an erection, the radius of the inner cylinder increases, and the thickness of the outer cylinder decreases. This implies that the distance between the blood compartment and the environment decreases.

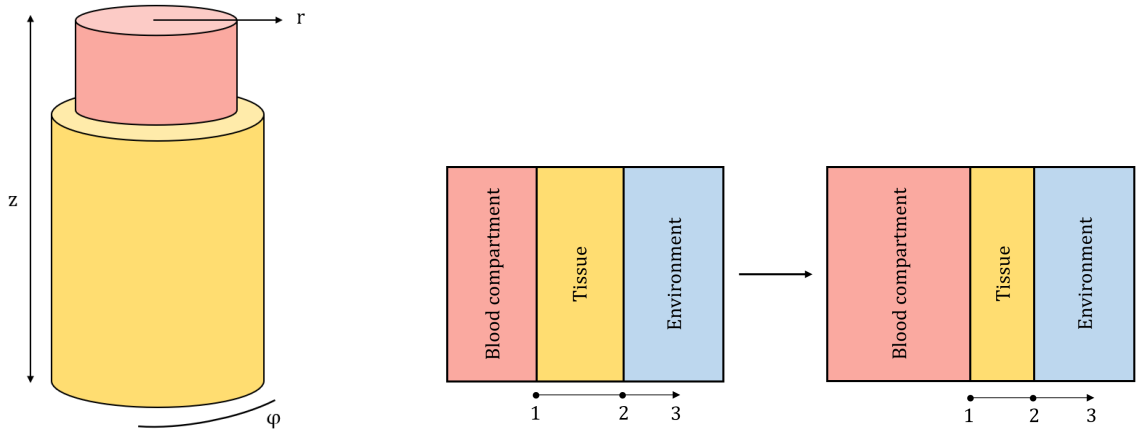

(a) *Cylinder with r, φ and z coordinates.* ***(b)*** *Cross-section of flaccid (left) and erect (right) condition.*

Figure 3: *Schematic view of heat transfer course which is described in our model. When the model changes from flaccid to erect state, the radius of the blood compartment increases and the thickness of the tissue decreases.*

3.2 Conduction

3.2.1 Heat diffusion equation

For this problem, a representation of the temperature distribution is desired, which describes how the temperature varies depending on the position in the medium. The heat flow in any location can be described in the direction of r, φ and z. The general form of the cylindrical heat diffusion equation according to Fourier's law is stated below [35].

$$\frac{1}{r}\frac{\partial}{\partial r}\left(kr\frac{\partial T}{\partial r}\right)+\frac{1}{r^2}\frac{\partial}{\partial \varphi}\left(k\frac{\partial T}{\partial \varphi}\right)+\frac{\partial}{\partial z}\left(k\frac{\partial T}{\partial z}\right)+\dot{q}=\rho c_p\frac{\partial T}{\partial t} \tag{3}$$

The thermal conductivity is described by k $[J/msK]$ (or $[W/mK]$) and the temperature by T $[K]$. On the right side of the equals term, the time-dependent term is given, with the mass density ρ $[kg/m^3]$, the specific heat at a constant pressure c_p $[J/kgK]$ and the time t $[s]$. The heat generation per unit volume is described by $\dot{q}$ $[W/m^3]$. As described in section 3.1, the heat transfer will be described in the r-direction and there is a steady state, steady flow condition. Furthermore, the amount of heat of the system during an erection increases due to an increase in blood volume. So, no additional heat is generated. Therefore, the term $\dot{q}$ is zero. This leaves us with the following differential equation.

$$\frac{1}{r}\frac{\partial}{\partial r}\left(kr\frac{\partial T}{\partial r}\right)=0 \tag{4}$$

3.2.2 Conductive temperature profile

In the connective tissue, conduction is the most prominent mechanism of heat transfer. In this section, the focus lays on the temperature gradient $(T_1 - T_2)$ between the radius of the blood compartment $(r_1$ $[m])$ and the radius of the skin surface $(r_2$ $[m])$. See Figure 4.

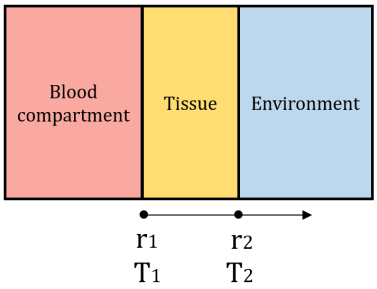

Figure 4: *Schematic view of the blood-tissue-environment interface in the direction of the radius (r). Conduction takes place mainly between radius 1 (r_1) and radius 2 (r_2).*

In our model, a steady state 1D heat conduction in a cylindrical body without sources is described. When solving equation (4), two boundary conditions are necessary, since it is a second order differential equation. The two boundary conditions are the following:

$$\text{Boundary condition 1: } T(r_1) = T_1 \tag{5}$$

$$\text{Boundary condition 2: } T(r_2) = T_2 \tag{6}$$

With the help of separation and integration, an expression for the temperature can be derived.

$$\int \partial\left(kr\frac{\partial T}{\partial r}\right) = \int 0 \cdot r \cdot \partial r \tag{7}$$

$$kr\frac{\partial T}{\partial r} = C_1 \tag{8}$$

$$\frac{\partial T}{\partial r} = \frac{C_1}{kr} \tag{9}$$

$$\int \partial T = \int \frac{C_1}{kr}\partial r \tag{10}$$

$$T = \frac{C_1}{k}ln(r) + C_2 \tag{11}$$

Fill in boundary conditions 1 and 2, and substitute to find expressions for the constants of integration:

$$C_1 = \frac{k(T_1 - T_2)}{ln(\frac{r_1}{r_2})} = \frac{k(T_2 - T_1)}{ln(\frac{r_2}{r_1})} \tag{12}$$

$$C_2 = T_1 - \frac{k(T_1 - T_2)}{ln(\frac{r_1}{r_2})}ln(r_1) = T_1 - \frac{k(T_2 - T_1)}{ln(\frac{r_2}{r_1})}ln(r_1) \tag{13}$$

Fill in the expressions for C_1 and C_2 in equation (11) to find the equation for the temperature as a function of the radius in steady state conduction, see equation (14). Values for r_2 can be calculated from known circumference values from the literature. Values for r_1 are less straightforward. The thickness of the skin and underlying fascias is measured three times during surgical correction of penile curvature due to Peyronie's disease in the St. Antonius hospital Nieuwegein. Besides, the thickness of the tunica albuginea has been described in different studies [36, 37]. Together, this led to a fair estimation of r_1 during flaccid state and erect state, see Appendix B.

$$T = T_1 + \frac{T_2 - T_1}{ln(\frac{r_2}{r_1})}ln\left(\frac{r}{r_1}\right) \tag{14}$$

3.2.3 Conductive heat flow

The general equation for the conductive heat flow $\dot{Q}_{cond}$ [W] through a cylindrical medium in the r-direction of is given below in equation (15) [35]. The minus sign is a consequence of the heat that is being transferred in the direction of decreasing temperature. In equation (16), the derivative of equation (14) is given.

$$\dot{Q}_{cond} = -kA\frac{dT(r)}{dr} \tag{15}$$

$$\frac{dT(r)}{dr} = \frac{T_2 - T_1}{ln(\frac{r_2}{r_1})}\frac{1}{r} \tag{16}$$

In our cylinder, the area (A) can be described as $2\pi rL$. Substitute equation (16) in equation (15):

$$\dot{Q}_{cond} = k2\pi L\frac{T_1 - T_2}{ln(\frac{r_2}{r_1})} \tag{17}$$

3.2.4 Conductive resistance

From the heat flow equation above, the resistance can be derived. The heat flow is defined by the temperature difference (ΔT $[K]$) divided by the conductive thermal resistance (R_{cond} $[K/W]$). Consequently, the conductive thermal resistance is the following:

$$R_{cond} = \frac{1}{k}\frac{1}{2\pi L} ln\left(\frac{r_2}{r_1}\right) \tag{18}$$

3.3 Convection

3.3.1 Newton's law of cooling

Heat flow by convection ($\dot{Q}_{conv}$ [W]) is described Newton's law of cooling (see equation (19) and (20)) [34]. The convective heat transfer coefficient is described by h $[W/m^2K]$, which depends on parameters like the type of medium and the flow velocity. The area of the surface is described by A $[m^2]$, the surface temperature is T_s $[K]$ and the temperature of the environment fluid is T_∞ $[K]$.

$$\dot{Q}_{conv} = hA(T_s - T_\infty) \tag{19}$$

$$q'' = h(T_s - T_\infty) \tag{20}$$

Here, q'' describes the heat flux per unit area $[W/m^2]$. From Newton's law of cooling, the convective thermal resistance (R_{conv} $[K/W]$) follows. Since our model describes a cylinder, the area (A) is defined as $2\pi r_{conv}L$.

$$R_{conv} = \frac{T_s - T_\infty}{\dot{Q}_{conv}} = \frac{T_s - T_\infty}{hA(T_s - T_\infty)} = \frac{1}{hA} = \frac{1}{h2\pi r_{conv}L} \tag{21}$$

3.3.2 Convective temperature profile

At the skin-environment interface, the main mechanism of heat transfer changes from conduction to convection. However, in the area directly to the wall it is stated that the velocity drops to zero (the so-called non-slip condition), where the Fourier law still applies [38]. Within this layer, the local surface heat flux is described by the equation below [38].

$$q_s'' = -k_f \left.\frac{\partial T}{\partial r}\right|_{r=r_2} \tag{22}$$

The s in q_s'' indicates the heat flux at the surface $[W/m^2]$, and k_f the thermal conductivity of the fluid (i.e. air) $[W/mK]$. The notation $r = r_2$ is used to refer to the skin surface, see Figure 4. An expression for h is obtained when equation (20) and (22) are combined [38].

$$h = \frac{\left.-k_f \partial T/\partial r\right|_{r=r_2}}{T_s - T_\infty} \tag{23}$$

An expression for the temperature at $r = r_2$ can be found when the first order differential equation above is solved. Boundary condition $T(r = r_2) = T_s$ is used.

$$\frac{h}{-k_f} = \frac{1}{T - T_\infty}\frac{\partial T}{\partial r} \tag{24}$$

$$\int \frac{h}{-k_f}\partial r = \int \frac{1}{T - T_\infty}\partial T \tag{25}$$

$$\frac{hr}{-k_f} + C = ln(T - T_\infty) \tag{26}$$

$$T = T_\infty + Ce^{\frac{-hr}{k_f}} \tag{27}$$

Find an expression for the constant of integration C with the help of the boundary condition,

$$C = T_s - T_\infty \tag{28}$$

which leads to the expression for the temperature as a function of r.

$$T = T_\infty + e^{\frac{-hr}{k_f}} (T_s - T_\infty) \tag{29}$$

Note that equation (29) is an approximation of the temperature distribution around $r = r_2$. Since $\frac{h}{k_f}$ is not constant over the r domain, this formula does not provide a representative temperature gradient for the convection.

3.3.3 Experiment - heat transfer coefficient

The air layer around the skin can be seen as an additional resistance of the heat flow from the body towards the environment. In order to calculate the heat flow through this resistance, we first need to estimate the convective heat transfer coefficient (h) with the help of an experiment. For this experiment, two digital temperature sensors (WINGONEER digital LCD thermometer, precision 0.1°C), an aluminium bottle filled with water, a cotton cloth and blanket were used. Properties of the bottle are listed in Table 1. The aluminium bottle was filled with warm water. Due to the high conductive properties of the aluminium (thermal conductivity, $k = 237\ W/mK$ [39]), the bottle has a negligible effect on the heat transfer of the water towards the environment. It is assumed that the heat distribution in the water is uniform. One thermometer was placed into the water and a second thermometer in the direct environment. The temperature of the water and environment over time were monitored in three different situations: 1) bottle in the open air, 2) bottle with cotton cloth in the open air, 3) bottle with cotton cloth and blanket. A delta temperature decrease of 2 °C was monitored, from either 34 °C to 32 °C or from 36 °C to 34 °C. The experiment was conducted three times. In Figure 5, graphs of the temperature decay as a function of time during one of the experiments are shown. Note that a Savitsky-Golay filter is applied to the data, which explains the smooth graph.

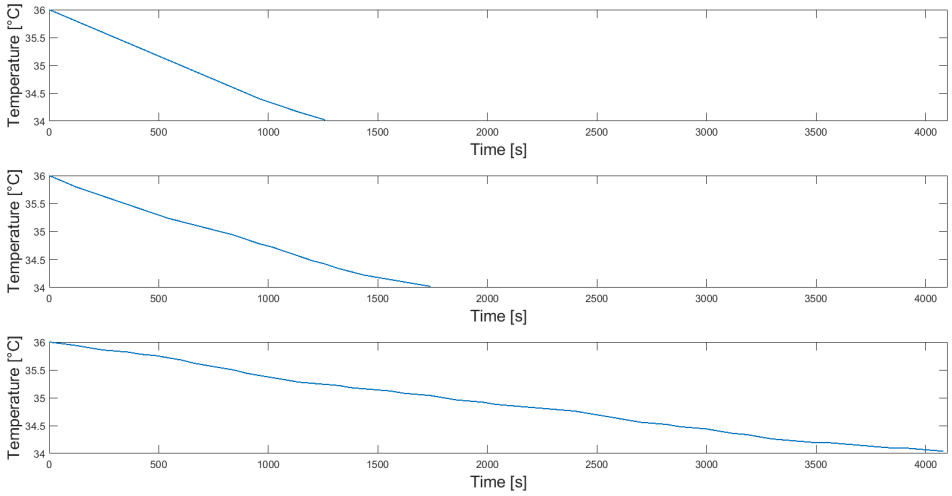

Figure 5: *The decrease in water temperature over time for three situations (from top to bottom): 1) bottle in the open air, 2) bottle with cotton cloth in the open air, and 3) bottle with cotton cloth and blanket. A Savitsky-Golay filter is applied to the data.*

Now, values for convective heat transfer coefficient h can be derived. During the experiment, the heat transfer out of the water bottle equals the increase in energy of the environment (law of conservation of energy) [34]. It follows that:

$$hA(T_i - T_\infty)dt = mc_p dT \tag{30}$$

The initial temperature T_i $[K]$ of the water, and thus the surface of the bottle, was either 307 K (34 °C) or 309 K (36 °C). The mass of the water will be described as $m = \rho V$ and the $dT = d(T - T_\infty)$. Substitute and rearrange,

$$\frac{d(T-T_\infty)}{(T_i-T_\infty)} = \frac{hA}{\rho V c_p} dt \tag{31}$$

then integrate to find the following expression.

$$ln\left(\frac{T(t)-T_\infty}{T_i-T_\infty}\right) = \frac{hA}{\rho V c_p} t \tag{32}$$

$$\frac{T(t)-T_\infty}{T_i-T_\infty} = e^{-bt} \text{ with } b = \frac{hA}{\rho V c_p} \tag{33}$$

During the experiments, the water temperature $T(t)$ $[K]$ and the time t $[s]$ are obtained. Values for the environment temperature T_∞ $[K]$, the initial temperature of the water T_i $[K]$, the area of the bottle A $[m^2]$, the density of water ρ $[kg/m^3]$, the volume of the water and bottle V $[m^3]$, and specific heat capacity of water c_p $[J/kgK]$ are given in Table 1.

Table 1: *Constants. The temperatures with an asterisk were monitored during each experiment.*

Parameter	**Symbol**	**Value**
Mean environment temperature* Experiment 1	T_∞	$299K$ no blanket $301K$ blanket
Mean environment temperature* Experiment 2	T_∞	$297K$ no blanket $301K$ blanket
Mean environment temperature* Experiment 3	T_∞	$298K$ no blanket $302K$ blanket
Initial temperature	T_i	$307K$ or $309K$
Area of bottle	A	$4.35 \cdot 10^{-2} m^2$
Density of water	ρ	$997 kg/m^3$
Volume of the bottle	V	$8.00 \cdot 10^{-4} m^3$
Specific heat capacity of water at 305 K	c_p	$4178 J/kgK$ [40]

With these constants and the information from Figure 5, values for b and thus for h can be calculated. The convective heat transfer coefficient, h, is calculated over the time for each experiment, see the graphs in Figure 6. During the measurement with cotton cloth and blanket, it took the longest to reach a delta temperature decrease of 2 $°C$, which is visible in Figure 5. Therefore, we also have more values for h in measurement 3 (Figure 6), since there are more data points. According to the book Fundamentals of heat and mass transfer by Bergman [34], the convective heat transfer coefficient in case of free convection is between 2-25 W/m^2K. This corresponds with the findings from our experiment. In Table 2, an overview of the mean convective heat transfer coefficients from the three experiments is given.

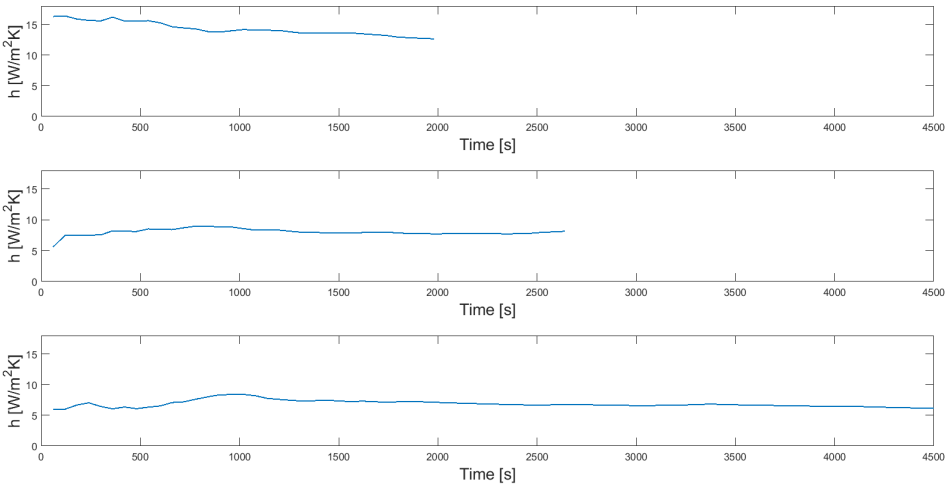

Figure 6: *The convective heat transfer coefficient (h) over time for three situations (from top to bottom): 1) bottle in the open air, 2) bottle with cotton cloth in the open air, 3) bottle with cotton cloth and blanket.*

Table 2: *Mean convective heat transfer coefficients (h $[W/m^2K]$) and their standard deviations (SD). In the bottom row, the overall mean is given.*

	Open air $[W/m^2K]$	**Cotton cloth** $[W/m^2K]$	**Cotton cloth and blanket** $[W/m^2K]$
h, experiment 1	14.3 (SD 1.1)	8.0 (SD 0.5)	6.9 (SD 0.6)
h, experiment 2	11.0 (SD 0.2)	8.8 (SD 0.7)	5.4 (SD 0.3)
h, experiment 3	10.0 (SD 0.6)	8.0 (SD 0.6)	6.4 (SD 0.4)
Mean h	11.8	8.3	6.2

3.4 Model outcomes

In Table 3, a summary of the equations that are derived in section 3.2 and section 3.3 is given. With these equations, the information from the experiment (section 3.3.3) and physiological parameters (see Appendix B), further calculations can be done.

Table 3: *Summary of conduction and convection equations.*

	Conduction	**Convection**
	Heat diffusion equation [35] $\frac{1}{r}\frac{\partial}{\partial r}\left(kr\frac{\partial T}{\partial r}\right)=0$	Newton's law of cooling [34] $\dot{Q}_{conv}=hA(T_s-T_\infty)$ $h=\frac{-k_f\partial T/\partial r\Big\vert_{r=r_2}}{T_s-T_\infty}$
Expression for the temperature	$T=T_1+\frac{T_2-T_1}{ln(\frac{r_2}{r_1})}ln\left(\frac{r}{r_1}\right)$	$T(r=r_2)=T_\infty+e^{\frac{-hr}{k_f}}(T_s-T_\infty)$
Heat transfer	$\dot{Q}_{cond}=k2\pi L\frac{T_1-T_2}{ln(\frac{r_2}{r_1})}$	$\dot{Q}_{conv}=h2\pi r_{conv}L(T_s-T_\infty)$
Resistance	$R_{cond}=\frac{1}{k}\frac{1}{2\pi L}ln\left(\frac{r_2}{r_1}\right)$	$R_{conv}=\frac{1}{h2\pi r_{conv}L}$

It is assumed that the temperature distribution in the blood compartment is homogeneous, so the main heat transfer occurs from the outer layer of the blood compartment ($T_1 = 37°C = 310K$) to the environment (T_∞). The temperature of the skin surface (T_s) is unknown. First, the complete resistance from the blood compartment towards the environment is determined. The total thermal resistance (R_{tot}) can be determined by a sum of all the resistances.

$$R_{tot}=R_{cond}+R_{conv}=\frac{1}{k}\frac{1}{2\pi L}ln\left(\frac{r_2}{r_1}\right)+\frac{1}{h2\pi r_{conv}L} \tag{34}$$

In Table 4, an overview of the total resistances are given in six different situations, 1) bare skin (naked) in flaccid condition, 2) flaccid penis with clothes and without blanket, 3) flaccid penis with clothes and blanket, 4) bare skin (naked) during an erection, 5) erect penis with clothes and without blanket, 6) erect penis with clothes and blanket. The total heat flow from the blood compartment towards the environment can be calculated with equation (1), see Table 4 for the results.

Table 4: *Total resistance and the total heat flow through the connective tissue to the environment.*

	Flaccid penis	**Erect penis**
Total resistance, $R_{th,tot}$		
Naked	5.2 K/W	2.7 K/W
Clothes	7.0 K/W	3.8 K/W
Clothes + blanket	9.0 K/W	4.9 K/W
Total heat flow, $\dot{Q}_{tot}$		
Naked	3.3 W	6.2 W
Clothes	2.4 W	4.5 W
Clothes + blanket	1.0 W	1.8 W

Next, we will determine the skin temperature in different conditions. According to the law of conservation of energy, the heat flow through the connective tissue (by conduction) equals the heat flow from the skin surface towards the environment (by convection). Thus, $\dot{Q}_{cond} = \dot{Q}_{conv}$ [34]. We will use the heat transfer equations from Table 3 to find an expression for the skin temperature. Note that $T_2 = T_s$.

$$k2\pi L\frac{T_1 - T_s}{ln(\frac{r_2}{r_1})} = h2\pi r_{conv}L(T_s - T_\infty) \tag{35}$$

$$\frac{T_1 - T_s}{T_s - T_\infty} = \frac{hr_{conv}}{k}ln\left(\frac{r_2}{r_1}\right) \tag{36}$$

Replace $X = \frac{hr_{conv}}{k}ln(\frac{r_2}{r_1})$ and find an expression for T_s.

$$T_1 - T_s = X(T_s - T_\infty) \tag{37}$$

$$T_s = T_1 - X(T_s - T_\infty) \tag{38}$$

$$T_s + XT_s = T_1 + XT_\infty \tag{39}$$

$$T_s(1 + X) = T_1 + XT_\infty \tag{40}$$

$$T_s = \frac{T_1 + XT_\infty}{(1 + X)} \text{ with } X = \frac{hr_{conv}}{k}ln\left(\frac{r_2}{r_1}\right) \tag{41}$$

The T_s for the six different conditions can be seen in Table 5. Due to the precision of 0.1°C of our temperature sensor, we round to one decimal. When naked, there is a ΔT of 1.4°C between the flaccid and erect state. For clothes (i.e. cotton underwear) and clothes plus blanket, there is a ΔT of 1.1°C and 0.4°C respectively. The outcome of our mathematical model comes close to the study of Kukkonen et al. (2010) [16], who found a penile skin temperature increase of 1.2°C in 30-45-year-old men who were naked.

Table 5: *Skin temperature in different conditions.*

	Flaccid penis	**Erect penis**	ΔT_s
Skin surface temperature, T_s			
Naked	306.9 K = 33.7 °C	308.3 K = 35.1 °C	1.4 °C
Clothes	307.8 K = 34.6 °C	308.8 K = 35.6 °C	1.1 °C
Clothes + blanket	309.1 K = 36.0 °C	309.6 K = 36.4 °C	0.4 °C

4 Methods

Due to a delay in the production process of the demo model of the wireless temperature sensor, we were unable to start with the study in healthy subjects. Therefore, SRE measurements were conducted in one healthy subject (age 28) with a commercially available thermistor. Penile skin temperature was monitored by the thermistor and tumescence plus rigidity simultaneously with the RigiScan during sleep. The goal was to compare at least 20 events (i.e. SREs) that were recognized by the RigiScan, with the temperature data.

4.1 Materials

Circumference (or tumescence) and rigidity were monitored by the RigiScan (GOTOP Medical Inc., St. Paul, Minnesota, USA), see Figure 7a. The penile skin temperature was monitored by the TM-220 thermistor (see Figure 7b) and accompanying TA-220 control module with LabScribe software from the iWorx Human Physiology kit (iWorx Systems inc, Dover, USA). Due to a lack of time, this sensor was best on short notice. The TM-220 thermistor has a negative temperature coefficient (NTC). This implies that the resistance of the material decreases with an increase in temperature and vice versa. Specifications of the TM-220 and TA-220 can be found in Appendix C. Furthermore, skin tape and a leg strap were used to attach the two sensors. The test subject wore cotton underwear and slept under a cotton blanket.

(a) *RigiScan Plus [41]. The loop cable with the blue mark was placed around the base of the penis, and the other loop cable under the glans penis. The computer was attached to the upper leg with the leg strap.*

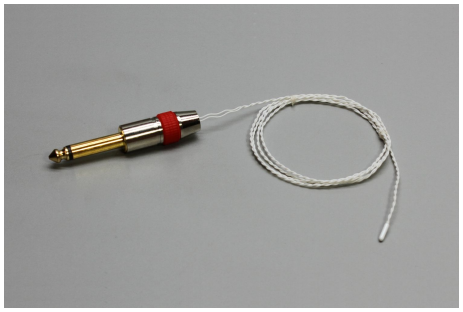

(b) *iWorx TM-220 thermistor [42]. The connector, visible on the left, was inserted to the iWorx TA-220 control module. The cone-shaped thermistor was placed on the lateral side of penile shaft with skin tape.*

Figure 7: *The two sensing systems.*

4.2 Protocol

In the evening prior to the measurement, the test subject was not allowed to drink alcoholic beverages or take any medication. Right before the healthy subject went to sleep, the RigiScan and leg strap were attached according to the manual. The RigiScan has two loop cables, the BASE and the TIP loop, which were placed around the proximal penile shaft and around the distal shaft (under the glans penis) respectively. The thermistor was attached to the skin on the lateral side of the penis with the help of skin tape. The lateral side of the penis was chosen to make sure the temperature was monitored as closely as possible to one of the corpora cavernosa. small pieces of skin tape were used to attach the thermistor, and not placed as a band wrapped around the shaft to minimize discomfort. Both sensing systems were switched on simultaneously. The next morning, the sensing systems were switched off when the test subject woke up. The protocol was repeated until a total of 20 SREs were monitored by the RigiScan.

4.3 Data preparation

The RigiScan data was extracted as graphs and information that was calculated automatically by the RigiScan software. This information included the number of registered events, their duration, average tumescence, and rigidity. The duration of each erection was checked manually because the erections measured by the TIP loop and the BASE loop did not always correspond. Raw data from the thermistor was exported as a temperature vector and a time vector from the Labscribe software, with a predetermined sampling frequency of 200 Hz. Data analyses of the thermistor data were executed in Matlab R2018b. Statistical analyses were performed in SPSS version 27.

First, a low-pass filter was applied to remove high frequency noise, based on a periodogram. A cut-off frequency of 5 Hz was chosen since most of the frequency content was below this value. We saw that there was no sensor drift over an eight-hour temperature measurement of the room temperature during the daytime, implying that a high-pass filter was unnecessary. However, there seemed to be a low frequent sinus-like wave in the raw temperature data, which matched with the circadian temperature cycle. Several studies described the circadian cycle that the core body temperature follows by periodic variations in heat production and heat loss [43, 44, 45]. In a study of Krauchi et al. [43] (1994), a 34-hour monitoring of proximal skin temperature (thigh, infraclavicular region, and forehead) showed the same circadian rhythm as the core temperature. On the other hand, the temperature profiles of distal skin measurements (hands and feet) were in opposite phase. In our study, we correct for the circadian cycle by applying a high-pass filter with a cut-off frequency of 0.00003 Hz, which corresponds to a period of nine hours (cut-off frequency = 1 / period).

Second, time and temperature intervals from the temperature data were extracted. These intervals corresponded with erections regarding the outcomes from the RigiScan measurements. Although the duration of each event was computed automatically by the RigiScan software, we also calculated them manually based on the RigiScan graphs. For example, when an erection was seen in the RigiScan data from 03:05 AM - 03:25 AM, this interval was also extracted from the temperature data. This provided us a time and temperature vector for each event. Afterwards, the time and temperature vectors were assimilated, i.e. adjusted so that the time and temperature of each vector started at the same value. This step is visualised in Figure 8.

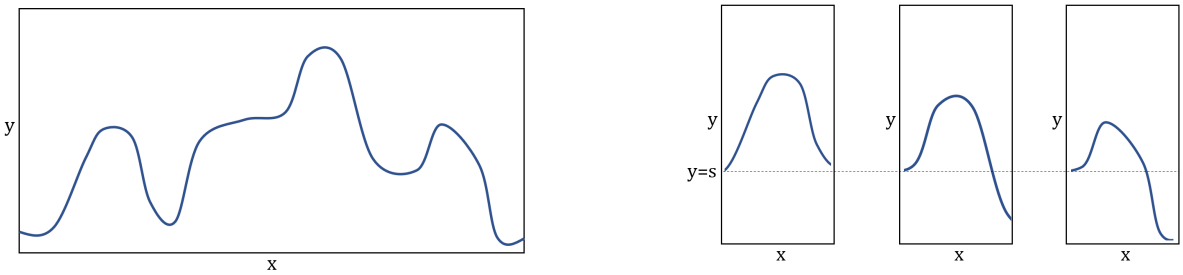

(a) *Example of thermistor data.* ***(b)*** *Separation and assimilation of intervals.*

Figure 8: *Example of data preparation. Suppose that the three peaks in* ***(a)*** *correspond to three hypothetical erections. Intervals were separated for each erection, and the time and temperature vectors were equated. In Figure* ***(b)*** *the intervals are equated to the line y=s and all start at x=0.*

Next, we classified the erection intervals by duration into three categories. Category 1 included the erection intervals from 5-15 minutes, category 2 the events of 16-25 minutes, and category 3 the events of 26 minutes and longer. This enabled us to analyse the relation between the duration of an erection and the variations in penile skin temperature.

4.4 Data analysis

All temperature data was plotted in the same graph. Medians and interquartile ranges were determined for fixed time steps, every 30 minutes. The mean tumescence was calculated from the average tumescence of the TIP and the BASE loop, which were both determined by the RigiScan software. When either the average tumescence of the TIP or the BASE was missing, the mean tumescence was the same as the non-missing value. For data that was distributed normally, means and standard deviations were calculated. For non-normal distributed data, on the other hand, we calculated medians and interquartile ranges.

The temperature at t = 0 from every event was plotted against the temperature after t = 10 minutes in a scatterplot. We chose this time step of 10 minutes because we observed in the RigiScan graphs that the peak tumescence was reached after 5-10 minutes in every erection. We assumed that peak tumescence indicates a full erection. Two studies demonstrated that the circumferential increase during an erection was closely followed by the temperature rise. [13, 18]. Therefore, we assumed that after approximately 10 minutes, a penile skin temperature increase should have taken place. The difference

between the temperature at t = 0 and t = 10 minutes was tested with the non-parametric Wilcoxon signed-rank test. Results were considered significant if $|Z| > 1.96$, $p < 0.05$. Under the null hypothesis (H_0): there is no difference in penile skin temperature between the start of the erection interval and after 10 minutes, $H_0 : T(t = 10) - T(t = 0) = 0$.

Next, we calculated the median temperatures and interquartile ranges at fixed time steps of all events together. Fixed time steps of 3 minutes were taken. Due to differences in the duration of the events, the number of data points decreased as we moved further along the time axis. The evaluation of the median temperature per time step presented an overview of the temperature gradient over time.

Furthermore, the slope of each erection interval was compared to slopes of temperature intervals when no erection took place. For each erection interval, an interval of the same number of samples previous to this erection interval was selected, with a gap of five minutes in between. This five-minute gap was chosen to make sure that there were no temperature processes already started that could have influenced the slope. In addition, slopes were also calculated for the first 10 minutes of each erection interval and non-erection interval. The selection of intervals is visualised in Figure 9. The slope of each interval was determined with the help of the first degree polynomial. The Wilcoxon signed-rank test was applied to determine if the slopes of the erection intervals and non-erection intervals were significantly different ($|Z| > 1.96$, $p < 0.05$). A non-parametric test was used since the data was not normally distributed. We have two null hypotheses (H_0). The first: there is no difference in slope between the erection intervals and the non-erection intervals, $H_0 : slope(erection) = slope(non - erection)$. And the second: there is no difference between the slopes of the first 10 minutes of the erection intervals and the slopes of the first 10 minutes of the non-erection intervals, $H_0 : slope(erection_{10}) = slope(non - erection_{10})$.

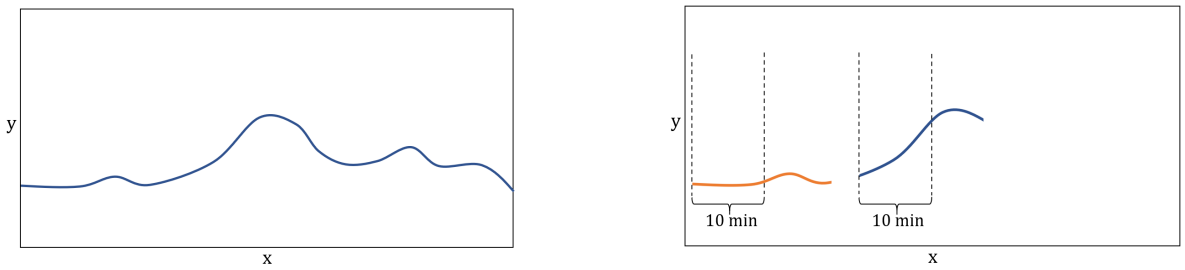

(a) *Example of thermistor data.*

(b) *selection of (10-minute) intervals.*

Figure 9: *Example of interval selection for slope analysis. Suppose that the peak in* ***(a)*** *corresponds to one hypothetical erection in the RigiScan data. In* ***(b)****, the orange graph is the non-erection interval with a five-minute gap before the erection interval (blue graph) starts. The orange and blue graphs have the same number of samples. Furthermore, the mean slopes of the first 10 minutes of both intervals are determined as well, marked by the dashed lines.*

5 Results

A total of 22 events (i.e. SREs) were monitored during 7 nights. Every measurement started around 10 PM and the sensing systems were switched off around 7 AM. In the RigiScan data, we see that most erections occur in the second half of the night. In Table 6, an overview of all events with their duration, average tumescence, and the average slope of the complete interval and the first 10 minutes is listed. Missing values of the average tumescence are caused by either a RigiScan error or a detached sensor loop. On the bottom, the mean and standard deviation or median and interquartile range are given, depending on the (non-)normal distribution of the data. The average duration of the erections that are measured in our healthy subject (mean = 25.4 minutes, SD = 12.8) corresponds to the average duration reported in the literature [46]. Figure 10a depicts an overview of all temperature data in one plot before the high-pass filter was applied. The penile skin temperature varies between 32 °C and 36 °C. In the first 30-60 minutes, a joint increase in temperature is seen in all measurements. The medians and interquartile ranges are calculated every 30 minutes and plotted in Figure 10b. An example of the RigiScan data from one measurement and its accompanying temperature data can be found in Appendix D.

Table 6: *This table provides an overview of the mean event duration, the average tumescence, and the slopes of the (10-minute) intervals. The event duration is determined based on a combination of RigiScan information and manual measurements from the raw data. The average tumescence is given by the RigiScan software. In several events either the TIP or BASE tumescence is missing, which was caused by a loose TIP loop (event 12, 18, 20, 21, 22) or an error in the measurements from the BASE loop (event 1-7). The Shapiro-Wilk test is used to test for normal distribution of the data. SD = standard deviation. IQR = interquartile range.*

Event no.	**Event duration** [min]	**Avg tum. TIP** [cm]	**Avg tum. BASE** [cm]	**Mean tum.** [cm]	**Slope, complete interval** [$°C/s$] $\cdot 10^{-5}$	**Slope, first 10 minutes** [$°C/s$] $\cdot 10^{-5}$
1	42	6.9	-	6.9	-10.2	14.0
2	60	7.1	-	7.1	4.3	82.2
3	18	9	-	9	-2.4	18.0
4	24	7.3	-	7.3	0.9	80.3
5	12	6.6	-	6.6	42.6	51.1
6	42	9.3	-	9.3	-2.2	53.2
7	9	9.0	-	9.0	30.4*	30.4*
8	24	7.4	7.0	7.2	-45.4	-1.5
9	42	5.6	6.4	6.0	16.2	13.0
10	15	7.7	6.9	7.3	-34.6	-1.2
11	42	5.6	6.8	6.2	34.7	-8.2
12	30	-	6.5	6.5	-15.2	7.5
13	15	8.2	6.9	7.6	-36.7	-52.3
14	24	8.7	6.4	7.6	-10.6	-48.1
15	21	8.6	6.4	7.5	2.8	92.2
16	21	7.2	6.2	6.7	-9.6	5.6
17	15	6.5	6.7	6.6	1.8	-18.1
18	15	-	6.0	6.0	10.4	6.8
19	15	6.3	6.2	6.3	49.6	43.6
20	27	-	6.1	6.1	83.1	160
21	21	-	6.2	6.2	81.6	49.5
22	24	-	6.3	6.3	60.9	78.7
Mean (SD) or Median (IQR)	25.4 (SD 12.8)	7.3 (IQR 2.1)	6.40 (IQR 0.6)	7.1 (SD 1.0)	2.3 (IQR 46.9)	16.0 (IQR 60.8)

* *Event no. 7 has a duration of 9 minutes. Therefore, the slope of the complete interval and the slope of the 10-minute interval are identical.*

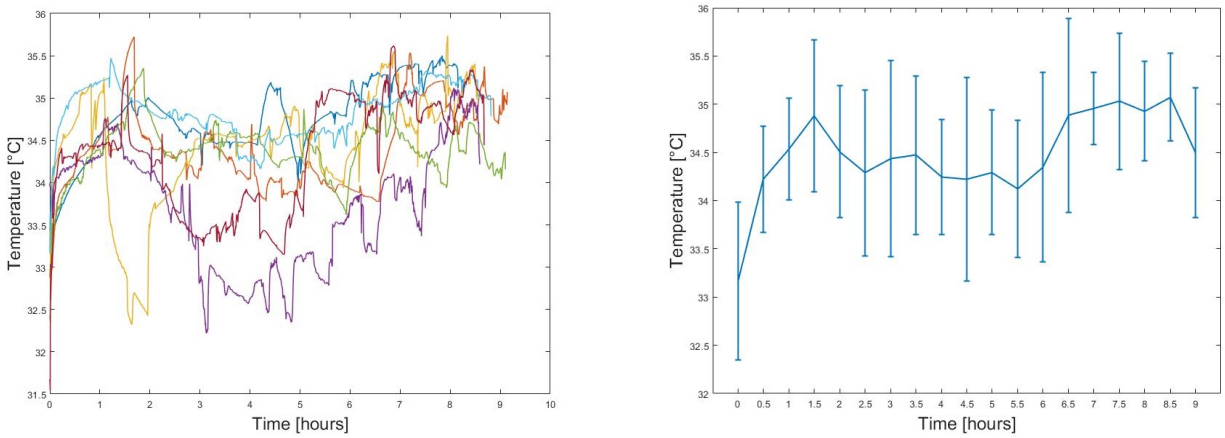

(a) *All temperature data.* ***(b)*** *Medians and interquartile ranges.*

Figure 10: *An overview of all temperature data in one plot. A low-pass filter was applied to cancel high frequency noise. In this plot, the high-pass filter is not applied to show the circadian rhythm. Figure* ***(a)*** *depicts the complete data of the seven temperature measurements. In* ***(b)*** *the median temperature and interquartile range are plotted every 30 minutes.*

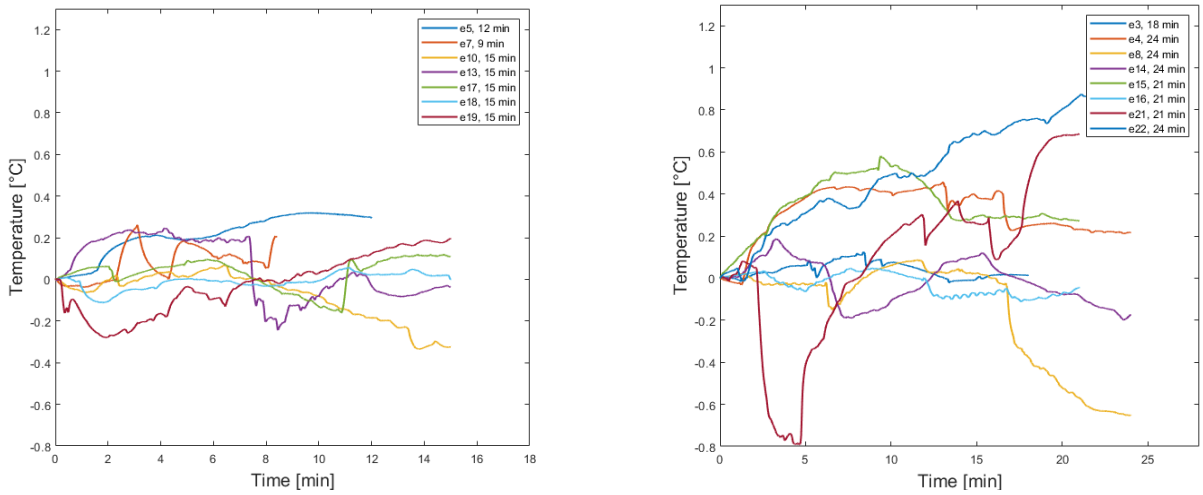

(a) *category 1: 5-15 minutes, n = 7.* ***(b)*** *category 2: 16-25 minutes, n = 8.*

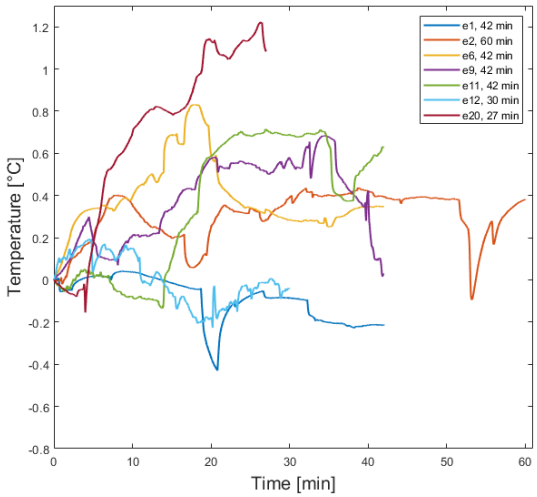

(c) *category 3: 26+ minutes, n = 7.*

Figure 11: *The 22 events divided over three categories based on their duration. The duration of every event is given in the legend. Every event starts at t = 0 minutes and T = 0 °C. The y-axes are equal.*

In Figure 11 the events are plotted per category, starting at t = 0 minutes and T = 0 °C. Every category includes 7 or 8 events. The temperature profiles of the events seem more divergent in category 2 and 3, compared to category 1. All events are plotted separately in Appendix D. The temperature at t = 0 and t = 10 minutes from each event is visible in the scatterplot in Figure 12. Most of the data points are located above the dashed line. On average, the penile skin temperature is significantly higher at t=10 minutes (median = 0.170, IQR = 0.355) than at t=0 (median = 0.0147, IQR = 0.420), Z = -2.613, p = 0.009, r = -0.56. Therefore, the null hypothesis is rejected, $H_0 : T(t = 10) - T(t = 0) \neq 0$.

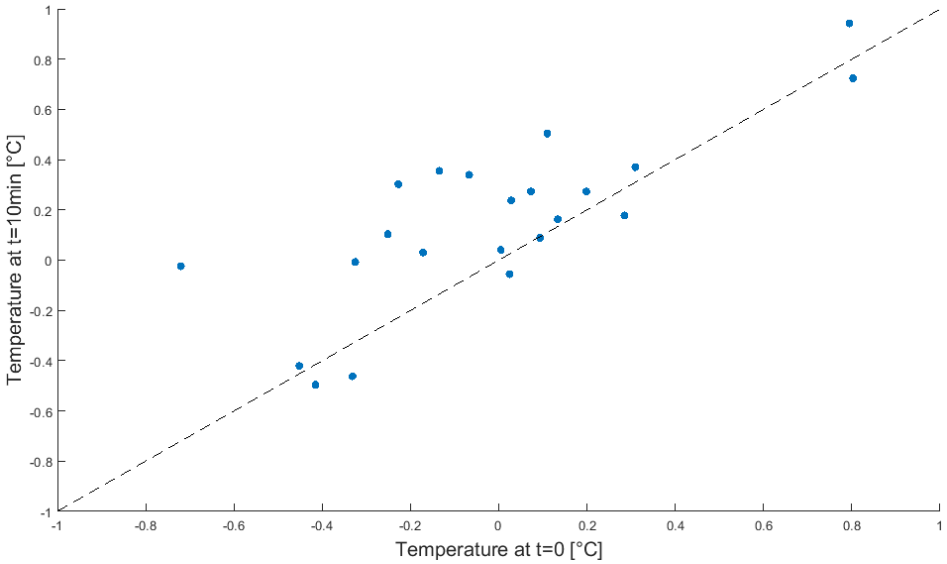

Figure 12: *Scatterplot with the temperature at $t = 0$ on the x-axis and the temperature at $t = 10$ minutes on the y-axis. Note that the high-pass filter was applied to the data, which explains the non-physiological temperatures. The dashed line is $y = x$. The dots above the dashed line indicate a higher temperature at $t = 10$ compared to its baseline value ($t = 0$). Contrarily, the dots below the dashed line indicate a lower temperature at $t = 10$.*

In Figure 13, the median temperature and its interquartile range of all events are plotted every three minutes. The number of samples decreases as we move along the x-axis. There is an increasing trend in temperature, but the interquartile ranges are higher than the medians. The median temperature is the highest at t = 33 minutes (n = 5, median = 0.40 °C, IQR = 0.43).

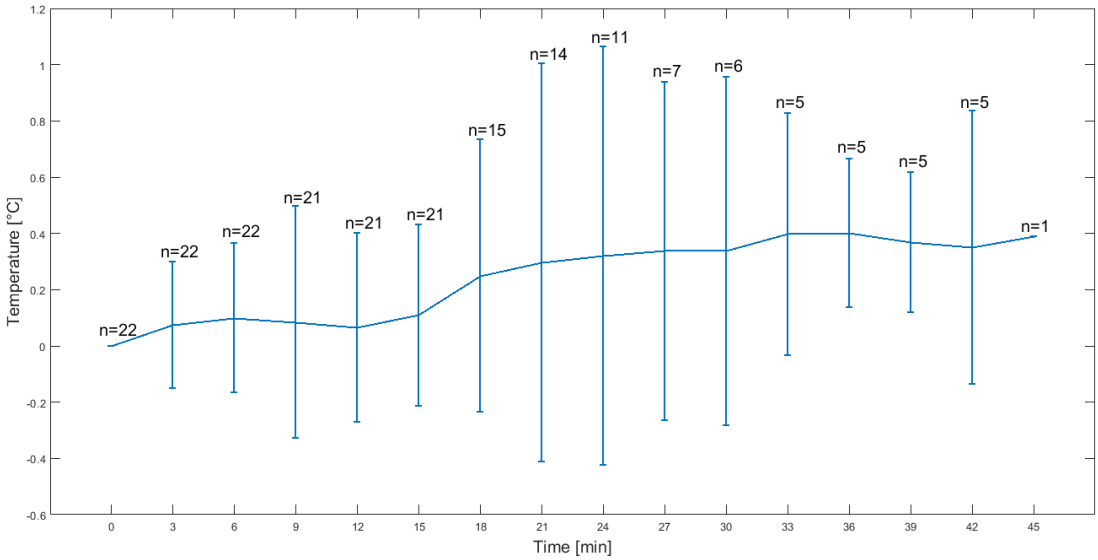

Figure 13: *The median temperature and its interquartile range every three minutes. The number of samples (n) is given at every time step. All events start at $t = 0$ and $T = 0$.*

In Table 7, the median slopes and interquartile ranges of the (non-)erection intervals and 10-minute intervals are given. In the same table, the outcomes from the non-parametric Wilcoxon signed-rank test are displayed. The slopes from the complete erection intervals (median = $2.29 \cdot 10^{-5}$ °C) are not significantly different from the non-erection intervals (median = $1.16 \cdot 10^{-5}$ °C), Z = -1.023, p = 0.306. Therefore, the null hypothesis is not rejected, $H_0 : slope(erection) = slope(non-erection)$. The slopes of the 10-minute erection intervals (median = $16.0 \cdot 10^{-5}$ °C) are again not significantly different from the slopes of the 10-minute non-erection intervals (median = $-2.91 \cdot 10^{-5}$ °C), Z = -1.542, p = 0.123. Thus, the null hypothesis of the 10-minute interval is also not rejected, $H_0 : slope(erection_{10}) = slope(non-erection_{10})$.

Table 7: *Median slopes and interquartile ranges (IQR) from the erection intervals and non-erection intervals. A Wilcoxon signed-rank test is applied. Differences are considered significant if $|Z| > 1.96$ or $p < 0.05$.*

	Complete interval		**10-Minute interval**	
	erection	*non-erection*	*erection*	*non-erection*
Median slope [°C/s]	$2.29 \cdot 10^{-5}$	$1.16 \cdot 10^{-5}$	$16.0 \cdot 10^{-5}$	$-2.91 \cdot 10^{-5}$
IQR	$46.9 \cdot 10^{-5}$	$31.9 \cdot 10^{-5}$	$60.8 \cdot 10^{-5}$	$33.4 \cdot 10^{-5}$
Z	-1.023		-1.542	
p	0.306		0.123	

6 Discussion

6.1 Discussion of the results

Our study shows that the temperature at t = 10 minutes is significantly higher compared to the baseline temperature (t = 0 minutes) during each erection interval. This suggests a skin temperature increase during the first 10 minutes of an erection. However, this result provides no information about the temperature gradient between t = 0 and t = 10 minutes. Although the temperature increase is significant, this concept is not suited for clinical practice yet. Contrary to expectations, we do not find a significant difference between the slopes from the intervals where an erection takes place (according to the RigiScan data) and the slopes from the intervals of the same length where no erection takes place. Making a difference between the complete interval and the first 10 minutes also does not affect the statistical proof. Yet, we do see an increase in mean slope when only the first 10 minutes of the erection interval are selected (median = $16.0 \cdot 10^{-5}$ °C/s), compared to the 10-minute non-erection interval (median = $-2.91 \cdot 10^{-5}$ °C/s). This quite obvious difference is pointing to a rising temperature during an erection. Unfortunately, the interquartile ranges are bigger than the temperature increase itself, which we also see in Figure 13. This supports the observation that our temperature data is disturbed by environment temperature fluctuations. These inconclusive results uncover the challenges of home monitoring.

We expected to see no sudden temperature variations during an erection interval. After all, SREs occur during periods of REM sleep, when the body is in complete muscle atonia [47]. The latter implies that the patient does not move during an erection (i.e. REM sleep). The graph in Figure 14a is an example of what we expected to see: a gradual increase in skin temperature, without sudden interruptions. Figure 14b, on the other hand, is an example of a quick temperature change that we did not expect to see during an erection interval. We also found a decreasing temperature gradient in some erection intervals. The reason for this rather contradictory result is still not clear. Most likely, the quick temperature change in event 14 (Figure 14b) was caused by movements of the body or a blanket. It is plausible that the bed partner caused blanket movements and this may have led to the quick temperature changes during erection intervals. Presumably, this factor is responsible for this result. We have to keep in mind that a patient who will sleep with a sensor that is very sensitive to environmental changes, may also undergo disturbances caused by the bed partner. Moreover, the small size of the thermistor could have led to imperfect skin-sensor contact. The latter results in a sensor that is more sensitive to environmental changes.

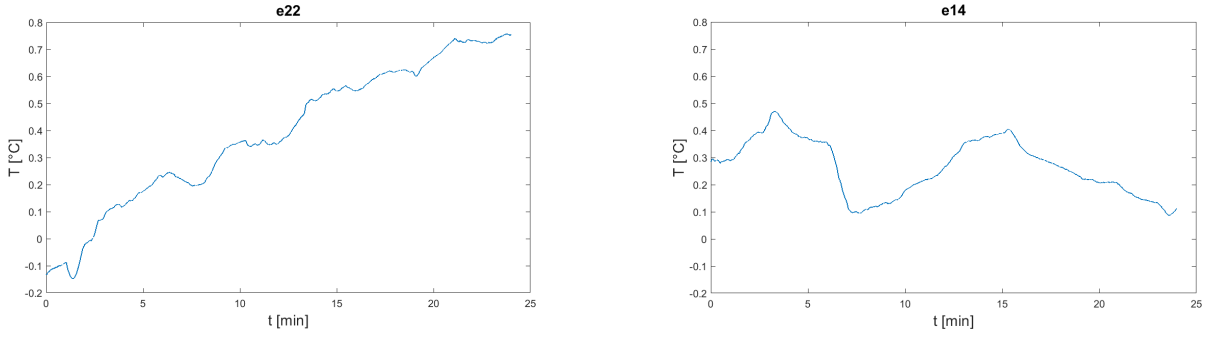

(a) *Event 22* ***(b)*** *Event 14*

Figure 14: *Two erection intervals. The x-axes and y-axes are equal.*

In our heat transfer model, the heat flow as a function of a changing circumference (and thus radius) is described. The circumferences implemented in our model were based on a meta-analysis [48]. The model demonstrates that an increase in skin temperature during an erection also occurs when the ambient temperature rises (due to the use of clothing and blankets). Furthermore, the ΔT between an erection and non-erection decreases when the ambient temperature increases, which is also in line with our expectations. Heat flows from a high temperature towards a low temperature [34]. The bigger the temperature difference, the bigger the heat flux. So, when the ambient temperature increases due to clothing or blankets, the heat flux decreases. This explains the lower ΔT between an erection and non-erection when the ambient temperature increases.

Theoretically, a circumferential increase can only be caused by the accumulation of blood in the corpora cavernosa. Therefore, a skin temperature increase occurs when the penile circumference increases. When the relation between the tumescence and accompanying skin temperature is better understood, this could be the main input parameter to validate our model. For instance, when patient X has a penile circumference that increases from 5 cm during the flaccid condition to 6.5 cm during an erection, the corresponding temperatures can be used to train our model. Unfortunately, we were not able to analyse the relation between temperature slope and tumescence, since the information provided by the RigiScan was not reliable. Moreover, age as an input parameter for such a model can also be considered in future research, since it was described that the penile skin temperature decreases with age [16].

Our study is a pilot study for further research. The biggest challenges of skin temperature measurements are to ensure adequate skin-sensor contact, and to rule out the effect of external factors (moving blankets, the heat of other body parts, body movements), or otherwise filter them out. In our exploratory study we chose to minimize data filtering as much as possible, to avoid losing physiological information. As described in the methods, a filter was applied to remove the circadian rhythm. Still, the results from the data analysis did not change before and after elimination of this circadian rhythm. In Figure 10, the sinus-like circadian rhythm is visible (before the high-pass filter was applied). This result indicates that we are able to measure a physiological phenomenon with the thermistor, and that our data is not completely distorted by ambient changes. Looking at Figure 10, a joint rise in each temperature measurement is seen during the first 30 minutes. This is explained by the fact that the healthy test subject went to bed right after the thermistor was attached and switched on. Therefore, the first 30 minutes are not representative for slope analysis in such measurements.

6.2 Strengths and limitations

An important strength of our study is that we are the first to describe the thermal changes during an erection in a model, and the first to monitor penile skin temperature during a night of sleep at home. The phenomenon of an increasing penile skin temperature during an erection is described in several studies [13, 14, 15, 16, 17, 18], only in laboratory conditions. In our study, an important step towards home monitoring of SREs with a new sensing system is made.

Another strength in favor of the temperature sensor is the outcome of our heat transfer model, which shows that a penile skin temperature increase occurs, despite the use of clothing and blankets. We set up a mathematical model without correction parameters and still calculated realistic outcomes. According to the outcomes of the model, the skin temperature varies between 33.7°C and 36.4°C (see Table 5), which comes close to the temperatures we have found in our measurements (see Figure 10). The 0.4°C as an outcome from our model matches the maximum of 0.4°C temperature rise in Figure 13. Moreover, a small temperature sensor for the monitoring of SREs increases the sleep comfort substantially, compared to the RigiScan. Especially since the size of the RigiScan device results in reduced freedom of movement. Furthermore, the BASE and TIP loop tighten every 15 seconds [8], which is not helpful for a natural night of sleep.

Given that our findings are based on a single healthy subject, the results from such analyses should therefore be treated with considerable caution. Nonetheless, an exploratory study in one subject brings advantages. For instance, an experiment with one healthy subject allows for constant test conditions, e.g. the thermal properties of the penile tissues are equal in each experiment, and clothes and blankets should give equal disturbance to the data in each measurement. However, experiments with a representative sample of the male population would allow for the implementation of the results to the average patient population. For example, an important aspect is the influence of age on penile skin temperature changes during an erection [16].

It is plausible that a number of limitations may have influenced the results obtained. To begin with, we did not include a reference thermistor in our measurement setup. A second thermistor that is placed on another body part, such as the thigh or hip, may assist in the understanding of fast temperature fluctuations. Second, the TM-220 thermistor not only measured the skin temperature, but also the environment temperature. The contact area with the skin was small and there was no sensor housing around the sensing element, which made it prone to pick up temperature fluctuations of the direct environment. Due to a lack of time, it was not possible to expand our measurement setup.

Another possible source of error was the performance of the RigiScan, which was rather disappointing. The average tumescence erroneously varied within one person. Also, it was expected to find approximately equal values for the TIP and BASE tumescence and rigidity. However, the graphs from the TIP loop and BASE loop did not always agree. This was probably a result of outdated software. Furthermore, a not working BASE loop and loosening TIP loop resulted in incomplete data in some measurements. All in all, one might wonder if a comparison with the RigiScan as being the golden standard is still is the best method. These observations add to a growing demand for a new method for measuring SREs.

Moreover, we need to take into account that our model assumes a constant ambient temperature and no influence of the rest of the body or moving blankets. Looking back on our experimental results, the step from our model to the experiments with the thermistor was perhaps too big, since this constant ambient temperature cannot be assured during home monitoring. Another assumption was that the heat distribution in the blood compartment (i.e. corpora cavernosa) was uniform. In reality, there will likely exist a temperature gradient from the middle of the corpora cavernosa towards the tunica albuginea. Likewise, the heat distribution from the proximal corpora towards the distal corpora is presumably not universal.

6.3 Recommendations for further research

Our first recommendation for future research is to add a second thermistor to the measurement setup, placed on the inner thigh or hip. If a new sensing system for monitoring SREs comes onto market someday, a second sensor is not favored. However, in this early stage of the study, this reference temperature sensor may help in better understanding the temperature profile of an erection. Another addition to the measurement setup can be a device that monitors the sleep stages, e.g. a watch or a smartphone application. A device that registers the REM sleep might be a useful addition, especially because the RigiScan has its flaws. Nonetheless, we have to be careful with watches and smartphone sleep apps, since there is an ongoing debate regarding their accuracy and role for clinical use [49, 50, 51].

Second, as described in the section above, the TM-220 thermistor had a small contact area with the skin and probably also measured the ambient temperature. We would therefore advise an isolating material as sensor housing around the sensor, to minimize measuring temperatures other than the penile skin. Then, we expect to see fewer (quick) temperature fluctuations. Furthermore, a bigger contact area is recommended to ensure good skin contact. Lastly, a wireless sensor for future research is advised to increase the freedom of movement, and thus increase sleep comfort.

Third, the goal of our heat transfer model was to investigate the influence of an alternating ambient temperature on the skin temperature in flaccid and erect conditions. Therefore, we described two states in our model: flaccid and erect. For a better understanding of the temperature profile, it may be interesting to model the skin temperature as a function of time. From the literature, we only know that the increase in penile skin temperature closely follows the circumferential increase in a laboratory setting [13, 18]. An important question is what the temperature profile looks like in home setting. Four students from the University of Twente made a start by studying the heating and cooling of the skin of the hand under several circumstances [52]. See Appendix E for a summary of their work. For further research, a mathematical description or phantom study of the temperature profile over time may support the analysis of experimental data from a study in healthy subjects.

Lastly, in a later stage of the study towards a new method for monitoring of SREs, it is recommended to investigate the influence of age on erections as well. Kukkonen et al. demonstrated that the penile skin temperature rise during an erection decreases with age [15, 16]. Possibly, in the older population, the temperature difference between flaccid and erect state is too small to distinguish itself from ambient temperature interference, especially when clothing and blankets come into play. Therefore, the combination of a temperature sensor with another sensor is an option that should be considered as well.

As mentioned in the Introduction, so far no one appears to study the continuous measurement of penile skin temperature at home for the monitoring of SREs. Therefore, there is no standardised method to analyse the obtained data. The importance of our results lies both in pioneering in this field and the search towards a worthy successor of the RigiScan in general.

7 Conclusion

In conclusion, a thermistor on itself is not able to distinguish SREs yet during home monitoring. According to our heat transfer model, a skin temperature rise does occur during an erection, even when the ambient temperature increases due to clothing and blankets. Furthermore, the results from our measurements with the RigiScan and thermistor suggested that a slight increase in penile skin temperature takes place during an erection. However, the statistical proof is poor. Probably, ambient temperature changes resulted in too much disturbance which influenced the data obtained. Therefore, an important issue to resolve for future studies is to minimize the influence of fast temperature fluctuations. All in all, it remains to be further clarified whether SREs monitored by the RigiScan and by skin temperature measurements correlate. We believe that our research will serve as a base for future studies in the development of a novel diagnostic device for ED.

References

[1] Wah-Yun Low, Chirk-Jenn Ng, Wan-Yuen Choo, and Hui-Meng Tan. How do men perceive erectile dysfunction and its treatment? a qualitative study on opinions of men. *The Aging Male*, 9(3):175–180, 2006.

[2] Faysal A Yafi, Lawrence Jenkins, Maarten Albersen, Giovanni Corona, Andrea M Isidori, Shari Goldfarb, Mario Maggi, Christian J Nelson, Sharon Parish, Andrea Salonia, et al. Erectile dysfunction. *Nature reviews Disease primers*, 2(1):1–20, 2016.

[3] NIH Consensus Conference. Impotence. consensus development panel on impotence. *The Journal of the American Medical Association*, (1):83–90, jul 1993.

[4] Ronald W Lewis, Kerstin S Fugl-Meyer, Giovanni Corona, Richard D Hayes, Edward O Laumann, Edson D Moreira Jr, Alessandra H Rellini, and Taylor Segraves. Definitions/epidemiology/risk factors for sexual dysfunction. *The journal of sexual medicine*, 7(4):1598–1607, 2010.

[5] Rany Shamloul and Hussein Ghanem. Erectile dysfunction. *The Lancet*, 381(9861):153–165, 2013.

[6] IA Aytac, JB McKinlay, RJ Krane, et al. The likely worldwide increase in erectile dysfunction between 1995 and 2025 and some possible policy consequences. *BJU international*, 84:50–56, 1999.

[7] RC Rosen, JC Cappelleri, MD Smith, J Lipsky, and BM Pena. Development and evaluation of an abridged, 5-item version of the international index of erectile function (iief-5) as a diagnostic tool for erectile dysfunction. *International journal of impotence research*, 11(6):319–326, 1999.

[8] William E Bradley, Gerald W Timm, Joan M Gallagher, and Bonnie K Johnson. New method for continuous measurement of nocturnal penile tumescence and rigidity. *Urology*, 26(1):4–9, 1985.

[9] Roos Edgar, Evelien J Trip, Gerjan JW Wolterink, Peter H Veltink, and Jack JH Beck. New methods for the monitoring of nocturnal erections. *International Journal of Impotence Research*, pages 1–7, 2020.

[10] Jia-Yi Dong, Yong-Hong Zhang, and Li-Qiang Qin. Erectile dysfunction and risk of cardiovascular disease: meta-analysis of prospective cohort studies. *Journal of the American College of Cardiology*, 58(13):1378–1385, 2011.

[11] Dimitrios Hatzichristou, Konstantinos Hatzimouratidis, Michael Bekas, Apostolos Apostolidis, Vasilios Tzortzis, and Konstantinos Yannakoyorgos. Diagnostic steps in the evaluation of patients with erectile dysfunction. *The Journal of urology*, 168(2):615–620, 2002.

[12] L Petrone, E Mannucci, G Corona, M Bartolini, G Forti, R Giommi, and M Maggi. Structured interview on erectile dysfunction (siedy©): a new, multidimensional instrument for quantification of pathogenetic issues on erectile dysfunction. *International journal of impotence research*, 15(3):210–220, 2003.

[13] Robert L Solnick and James E Birren. Age and male erectile responsiveness. *Archives of Sexual Behavior*, 6(1):1–9, 1977.

[14] Sabina Sarin, Rhonda Amsel, and Yitzchak M Binik. How hot is he? a psychophysiological and psychosocial examination of the arousal patterns of sexually functional and dysfunctional men. *The journal of sexual medicine*, 11(7):1725–1740, 2014.

[15] Tuuli M Kukkonen, Yitzchak M Binik, Rhonda Amsel, and Serge Carrier. Physiology: Thermography as a physiological measure of sexual arousal in both men and women. *The journal of sexual medicine*, 4(1):93–105, 2007.

[16] Tuuli M Kukkonen, Yitzchak M Binik, Rhonda Amsel, and Serge Carrier. An evaluation of the validity of thermography as a physiological measure of sexual arousal in a non-university adult sample. *Archives of sexual behavior*, 39(4):861–873, 2010.

[17] Jackie S Huberman, Samantha J Dawson, and Meredith L Chivers. Examining the time course of genital and subjective sexual responses in women and men with concurrent plethysmography and thermography. *Biological Psychology*, 129:359–369, 2017.

[18] Jeffrey S Webster and David Hammer. Thermistor measurement of male sexual arousal. *Psychophysiology*, 20(1):111–115, 1983.

[19] Karl-Erik Andersson and Gorm Wagner. Physiology of penile erection. *Physiological reviews*, 75(1):191–236, 1995.

[20] Albert C Leung, George J Christ, and Arnold Melman. Physiology of penile erection and pathophysiology of erectile dysfunction. In *Atlas of Male Sexual Dysfunction*, pages 1–25. Springer, 2004.

[21] Alan W Shindel and Tom F Lue. Physiology of erection. In *Cancer and sexual health*, pages 69–76. Springer, 2011.

[22] Ian Eardley. Pathophysiology of erectile dysfunction. *The British Journal of Diabetes & Vascular Disease*, 2(4):272–276, 2002.

[23] Daniel Udelson. Biomechanics of male erectile function. *Journal of The Royal Society Interface*, 4(17):1031–1048, 2007.

[24] Feng Qin, Liang Gao, Shengqiang Qian, Fudong Fu, Yang Yang, and Jiuhong Yuan. Advantages and limitations of sleep-related erection and rigidity monitoring: a review. *International Journal of Impotence Research*, 30(4):192–201, 2018.

[25] Francois A Giuliano, Olivier Rampin, Gerard Benoit, and Alain Jardin. Neural control of penile erection. *The Urologic clinics of North America*, 22(4):747–766, 1995.

[26] Mels F van Driel. Sleep related erections throughout the ages. *The journal of sexual medicine*, 11(7):1867–1875, 2014.

[27] Graham Jackson. The importance of risk factor reduction in erectile dysfunction. *Current Sexual Health Reports*, 4(3):114–117, 2007.

[28] Alessandro Serretti and Alberto Chiesa. A meta-analysis of sexual dysfunction in psychiatric patients taking antipsychotics. *International clinical psychopharmacology*, 26(3):130–140, 2011.

[29] Arthur Thomas, Christopher Woodard, Eric S Rovner, and Alan J Wein. Urologic complications of nonurologic medications. *The Urologic clinics of North America*, 30(1):123, 2003.

[30] Max Hirshkowitz, Ismet Karacan, Murat O Arcasoy, Guven Acik, Erdem M Narter, and Robert L Williams. Prevalence of sleep apnea in men with erectile dysfunction. *Urology*, 36(3):232–234, 1990.

[31] Carol A Holden, Robert I McLachlan, Marian Pitts, Robert Cumming, Gary Wittert, Johnathon P Ehsani, David M De Kretser, and David J Handelsman. Determinants of male reproductive health disorders: the men in australia telephone survey (mates). *BMC Public Health*, 10(1):1–9, 2010.

[32] F Hedon. Anxiety and erectile dysfunction: a global approach to ed enhances results and quality of life. *International Journal of Impotence Research*, 15(2):S16–S19, 2003.

[33] Walter F Boron and Emile L Boulpaep. *Medical physiology, Second edition*. Elsevier Health Sciences, 1237-1239, 2012.

[34] Theodore L Bergman, Frank P Incropera, David P DeWitt, and Adrienne S Lavine. *Fundamentals of heat and mass transfer, Seventh edition*. John Wiley & Sons, Ch.1, 2-31, 2011.

[35] Theodore L Bergman, Frank P Incropera, David P DeWitt, and Adrienne S Lavine. *Fundamentals of heat and mass transfer, Seventh edition*. John Wiley & Sons, Ch.2, 68-87, 2011.

[36] A Mander, G Palleschi, V Gentile, H Gezeroglou, T Dornbusch, AL Pastore, and A Carbone. Early echographical assessment of minimal lesions of cavernosum corpora and tunica albuginea in subjects with erectile dysfunction, suggestive of la peyronie's disease. *International journal of impotence research*, 18(6):517–521, 2006.

[37] Anthony J Edey, C Jason Wilkins, and Paul S Sidhu. *Clinical Ultrasound, third edition. Chapter 32 - Ultrasound of the penis*. Churchill Livingstone, 621-631, 2011.

[38] Theodore L Bergman, Frank P Incropera, David P DeWitt, and Adrienne S Lavine. *Fundamentals of heat and mass transfer, Seventh edition*. John Wiley & Sons, Ch.6, 378-383, 2011.

[39] Theodore L Bergman, Frank P Incropera, David P DeWitt, and Adrienne S Lavine. *Fundamentals of heat and mass transfer, Seventh edition*. John Wiley & Sons, Table A1, 983-986, 2011.

[40] Theodore L Bergman, Frank P Incropera, David P DeWitt, and Adrienne S Lavine. *Fundamentals of heat and mass transfer, Seventh edition*. John Wiley & Sons, Table A6, 1003-1004, 2011.

[41] Your Global Medical Equipment Platform MedWOW. Manufacturer specifications - rigiscan plus. Available from: http://www.medwow.com/med/erectile-dysfunction-analyzer/endocare/rigiscan-plus/64213.model-spec.

[42] iWorx Systems Inc. TM-220: Temperature sensor for the TA. Available from: https://iworx.com/products/sensors/tasensors/tm-220/.

[43] Kurt Krauchi and Anna Wirz-Justice. Circadian rhythm of heat production, heart rate, and skin and core temperature under unmasking conditions in men. *American Journal of Physiology-Regulatory, Integrative and Comparative Physiology*, 267(3):R819–R829, 1994.

[44] Jim Waterhouse, Barry Drust, Dietmar Weinert, Benjamin Edwards, Warren Gregson, Greg Atkinson, Shaoyuan Kao, Seika Aizawa, and Thomas Reilly. The circadian rhythm of core temperature: origin and some implications for exercise performance. *Chronobiology international*, 22(2):207–225, 2005.

[45] Dietmar Weinert and Jim Waterhouse. The circadian rhythm of core temperature: effects of physical activity and aging. *Physiology & behavior*, 90(2-3):246–256, 2007.

[46] Markus H Schmidt and Helmut S Schmidt. Sleep-related erections: neural mechanisms and clinical significance. *Current neurology and neuroscience reports*, 4(2):170–178, 2004.

[47] John Peever and Patrick M Fuller. The biology of rem sleep. *Current Biology*, 27(22):R1237–R1248, 2017.

[48] David Veale, Sarah Miles, Sally Bramley, Gordon Muir, and John Hodsoll. Am I normal? a systematic review and construction of nomograms for flaccid and erect penis length and circumference in up to 15 521 men. *BJU international*, 115(6):978–986, 2015.

[49] Sushanth Bhat, Ambra Ferraris, Divya Gupta, Mona Mozafarian, Vincent A DeBari, Neola Gushway-Henry, Satish P Gowda, Peter G Polos, Mitchell Rubinstein, Huzaifa Seidu, et al. Is there a clinical role for smartphone sleep apps? comparison of sleep cycle detection by a smartphone application to polysomnography. *Journal of Clinical Sleep Medicine*, 11(7):709–715, 2015.

[50] Adrian A Ong and M Boyd Gillespie. Overview of smartphone applications for sleep analysis. *World journal of otorhinolaryngology-head and neck surgery*, 2(1):45–49, 2016.

[51] Christopher P Lorenz and Adrian J Williams. Sleep apps: what role do they play in clinical medicine? *Current opinion in pulmonary medicine*, 23(6):512–516, 2017.

[52] Mathieu Broeders, Nina Hagen, Marit Kaptein, and Michelle van der Neut. Feeling hot: measuring skin temperature for diagnosing erectile dysfunction. thermistor for your mister: a research on measuring small skin temperature changes. *University of Twente, Bachelor thesis Technical Medicine*, 2021.

[53] Optum Inc. What is the normal temperature of blood? Available from: https://perks.optum.com/blog/what-is-the-normal-temperature-of-blood/.

[54] ITIS foundation. Thermal conductivity. Available from: https://itis.swiss/virtual-population/tissue-properties/database/thermal-conductivity/.

[55] iWorx Systems Inc. TA-220: Control module. Available from: https://www.iworx.com/documents/technotes/IX-TA-220.pdf.

[56] Andy Field. *Discovering statistics using SPSS, Third edition. Chapter 15: Non-parametric tests*. Sage, Ch. 15, 539-583, 2009.

A Perspective, International Journal of Impotence Research

IJIR: Your Sexual Medicine Journal
https://doi.org/10.1038/s41443-020-00365-9

PERSPECTIVE

New methods for the monitoring of nocturnal erections

Roos Edgar[1,2] · Evelien J. Trip[1,3] · Gerjan J. W. Wolterink[2,4] · Peter H. Veltink[2] · Jack J. H. Beck[1]

Received: 6 August 2020 / Revised: 22 September 2020 / Accepted: 8 October 2020

Abstract

The golden standard for measuring nocturnal erections is the RigiScan Plus. It is a relatively big and uncomfortable device dating from the previous century. The aim of this perspective is to conceptualize a user-friendly sensor that can be used at home for monitoring nocturnal erections. A literary search is carried out to explore the physiological changes during nocturnal tumescence and detumescence that can be measured non-invasively. Five sensor concepts are considered: plethysmography for penile arterial pulse, displacement sensor for axial length, strain gauges for radial rigidity and circumference, temperature sensors for measuring skin and cavernosal temperature, and a saturation sensor to measure hypoxia in cavernosal tissue during maximal rigidity. We think that due to practical issues, measuring penile length during sleep is impossible. Further research is recommended to investigate the remaining sensor concepts. Whether a combination of these techniques is favorable or only one of them should be studied more thoroughly.

Introduction

It is well known that the prevalence of erectile dysfunction (ED) increases with age, and ranges from 2 to 9% in men between 40 and 49 years old and increases up to 50–100% in the population older than 70 years [1]. According to the NIH Consensus Conference, ED is characterized as the inability to attain and/or maintain penile erection sufficient for satisfactory sexual performance [2]. Its cause can be either psychological, organic or mixed psychological and organic [1, 2]. A method to distinguish between a psychological and organic cause is by measuring a patient's nocturnal erections [1, 3]. Nocturnal penile erections are present in healthy men throughout their whole life and indicate an intact endocrine, vascular and neural supply as well as intact penile structures [1]. The golden standard for monitoring nocturnal erections and distinguish between psychogenic and organic causes is the RigiScan Plus (Dacomed Corporation, Minneapolis, Minnesota, USA) [3]. Due to several drawbacks of this device, a novel user-friendly device for home monitoring of nocturnal erections is requested. Therefore, the goal of this perspective is to conceptualize a sensor that can be used at home for monitoring nocturnal erections. The mode of action of the golden standard RigiScan is first described, followed by new concepts to measure nocturnal erections in the future.

The RigiScan Plus

The RigiScan Plus is the most widely accepted and one of the most reliable tools to differentiate organic from psychogenic causes [3]. Nocturnal penile erections occur during periods of rapid eye movement (REM) sleep [4]. The absence of nocturnal erections indicates an organic cause of ED and the presence of nocturnal erections indicates a normal penile function. The latter may imply a psychogenic cause [5]. The device registers the number and duration of nocturnal erections by monitoring the penile circumference and radial rigidity [6]. The apparatus is relatively big, uncomfortable and therefore disturbs a natural night of sleep. The sensor was developed in the previous century and its software is not updated to be compatible with the current operating systems on desktops, notebooks, tablets or smartphones. Therefore, new methods to measure and

✉ Jack J. H. Beck
j.beck@antoniusziekenhuis.nl

[1] Department of Urology, St. Antonius Hospital Nieuwegein, Utrecht, The Netherlands

[2] Department of Biomedical Signals and Systems (BSS), University of Twente, Enschede, The Netherlands

[3] Department of Gynaecology, St. Antonius Hospital Nieuwegein, Utrecht, The Netherlands

[4] Department of Robotics and Mechatronics (RAM), University of Twente, Enschede, The Netherlands

Published online: 21 October 2020

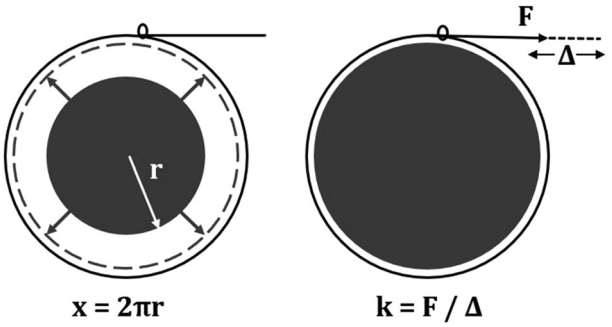

Fig. 1 Schematic view of loop cable to measure penile circumference and rigidity. The image on the left describes the calculation of the penile circumference by the position-sensing potentiometer. A change in x corresponds to a change in circumference (X_0 = initial penile circumference). The image on the right shows how the relative rigidity is determined with the help of the spring constant (k), which is analogous to the circumferential stiffness. Figure is adapted from Bradley et al. [9].

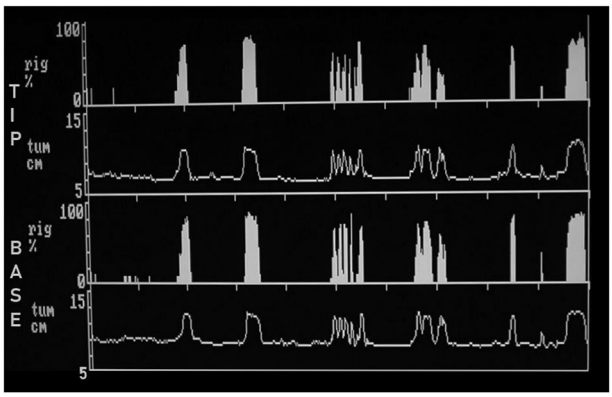

Fig. 2 Example of RigiScan data presentation during a nocturnal registration. The two graphs at the top are measured at the tip of the penis, and the two other graphs are measured at its base. On the x-axis, the time in hours is given. The y-axis of the first and third graph represent rigidity as a percentage. The y-axis of the second and fourth graph represent the tumescence in centimetres.

report nocturnal erections need to be developed. The RigiScan was developed by Bradley et al. for continuous measurement of nocturnal erections [7]. The device monitors penile rigidity and the tumescence of the penis expressed as circumference. The RigiScan consists of two nonelastic cable loops and a microcomputer for the processing of the data. The loop cables are attached to a position-sensing potentiometer and range from 5 to 15 cm circumference. Every fifteen seconds, the radial tumescence is measured by tightening the loops a little. This penile circumference is determined by the position-sensing potentiometer, which measures the change in x (Fig. 1). The change in the length of x relative to x_0 (the initial penile circumference) gives information about the actual penile circumference. A force of 1.1 N is sufficient for circumferential measurements [7].

Rigidity is monitored by means of the spring constant (k). A force (F) of 2.8 N results in a displacement (Δ) of the nonelastic loop cable. The spring constant (k) is analogous to the circumferential stiffness. The RigiScan device expresses the rigidity as a percentage relative to the spring constant of a semirigid rubber cylinder [7]. The material properties of this cylinder are not mentioned. We think they used a regular dildo to calibrate the RigiScan. We contacted GOTOP Medical, Inc. (Saint Paul, MN, USA) but our questions were not answered. A rigidity of 100% means that the penile rigidity is similar to the rigidity of the semirigid rubber cylinder [8]. A direct current torque motor pulls the loop cables every three minutes to determine the rigidity. When the penile circumference increases more than 3 mm, the rigidity sampling rate increases to once every 30 s [7]. The displacement of the loop is converted to a rigidity percentage. When the loop displaces ≥2.2 cm when a force of 2.8 N is applied, the rigidity is 0%. Zero displacement of the loop during a force of 2.8 N corresponds to a rigidity of 100%. For each 0.05 cm of loop displacement, the rigidity reduces by 2.3% [9]. Once connected to a computer with RigiScan Plus software a characteric graphic is plotted. See Fig. 2 for the measurement and presentation of normal nocturnal erections.

Possible measurable physiological changes during nocturnal erections

Arterial pulse

During nocturnal erections, dilation of the arteries in the early stage of erection reduces the vascular resistance and thereby increases the arterial flow into the corpora cavernosa. The flow increases from 2.5 ml/min in the flaccid state to 10–20 ml/min during the filling stage and decreases again when the intracavernosal pressure is increased [10]. This is accompanied by an increase in penile pulse amplitude, which is found by Bancroft et al. [11]. In most subjects, the increased penile pulse remained elevated throughout the increased penile circumference during erection. In other healthy subjects, however, the pulse amplitude declined during erection [11].

Rigidity

During maximal occlusion of the venous outflow, the intracavernosal pressure increases up to ~100 mmHg (the full erection phase). This pressure elevates further to the systolic blood pressure during maximal sexual arousal (the rigid-erection phase) [12]. The pressure in the corpus spongiosum, on the other hand, is only one-third to one half of the intracavernosal pressure [13]. This elevated outward

Table 1 Overview of consecutive physiological changes during erection, the accompanying noninvasive sensor principles and its advantages and disadvantages.

Physiological change	Noninvasive sensor principle	Advantages	Disadvantages
Neural innervation	Not available	X	X
Smooth muscle relaxation	Not available	X	X
Venous occlusion	Not available	X	X
Increase and decrease in arterial pulse	Photoelectric plethysmograph	Can monitor small vessels.	Changes in penile pulse have only been studied in small populations.
		Low cost.	Optimal site for sensor placement is unclear.
		High sensitivity.	
Increase in circumference	Radial strain gauge	Data can be easily interpreted, since it is comparable to the RigiScan data presentation.	Pressure on penile skin might disturb natural sleep.
		Provides information about duration and intensity of an erection.	
Increase in length	Resistive or capacitive displacement sensor	No pressure on penile skin is needed.	
		Different displacement sensors for medical applications already exist.	The influence of movement artefacts is unknown.
			Too many movable layers beneath the skin, so fixation is not possible.
Increase in rigidity	Multiple radial strain gauges with a different stiffness	Relation between percentage of rigidity and possibility of sexual intercourse is known [6].	Probably the least comfortable due to pressure on penile skin.
		Data can be easily interpreted, since it is comparable to the RigiScan data presentation.	Maximal acceptable pressure is unknown.
		Provides information about duration and intensity of an erection.	
Increase in cavernosal and skin temperature	Skin: thermocouple or thermistor	Small size of the sensor.	Little is known about:
		Applicable for young men, Δ2.4 °C of penile skin temperature.	Influence of external thermal factors and penile conductivity.
	Cavernosal: near infrared sensor seems an option	Minimal sleep disturbance, since no pressure on penile skin is needed.	Relation between temperature changes and duration and intensity of erection.
			Optimal site for sensor placement is unclear.
Decrease in oxygen saturation	Tissue oxygenation sensor	Small size of the sensor.	Little is known about:
		Minimal sleep disturbance.	Optimal site for sensor placement.
		Easy application.	Sensor settings for depth measurement.
			Relation between saturation levels and intensity of erection.

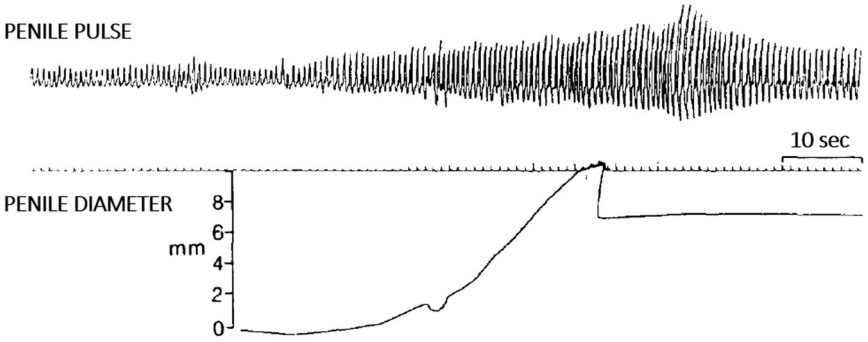

Fig. 3 Arterial pulse during erection, measured by a photoelectric plethysmograph. Figure is modified from Bancroft et al. [13].

pressure in the intracavernosal bodies results in an increased rigidity of the penile tissue. With an increased rigidity, the elasticity of the tissue decreases.

Circumference and length

A study of Promodu et al. shows that the mean penile base circumference of a flaccid penis increases from 9.14 cm to 11.5 cm in erect state. The mean penile length increases from ~8.21 cm to ~12.9 cm [14].

Temperature

Measurable elevations in skin temperature occur during sexual arousal caused by genital vasoconstriction [15]. A study in 1977 found a bigger change in temperature in the younger male population (19–30 years old), compared to males in the age of 48–65 years. The mean skin temperature increased from 33.8 to 36.2 °C (Δ2.4 °C) in the younger group and from 33.2 to 34.3 °C (Δ1.1 °C) among older men [16]. It is unknown whether the penis skin temperature depends on the thermal characteristics of the environment of the penis.

Oxygen saturation

In a study by Brow et al., saturation levels were monitored through a cavernosal blood gas analysis during a penile duplex ultrasonography in men with suspected impotence. They found a lower cavernosal PO2 as an indicator for impotence [17].

Possible sensor concepts to measure physiological changes during nocturnal erections

When developing a new sensing system, several requirements need to be met. Sensor requirements can be divided into technical aspects and user aspects. Technical aspects include reproducibility, accuracy, validity, linearity, precision, influence of environment and sampling rate. User aspects include comfort, donning and doffing time, safety, data presentation and battery capacity. The new sensor should not disturb the natural sleep pattern. The donning and doffing time should be maximal several minutes. Besides, the system should be able to monitor for minimal one or two nights (i.e., 24 h) consecutively before charging. Next to that, the data should be presented as graphs (similar to the RigiScan Plus), which can be interpreted by the physician and patient without difficulty. The results are also presented in Table 1.

Plethysmography for arterial pulse

Bancroft et al. showed that photoelectric measurements of an increased arterial pulse amplitude from the dorsal penile artery are correlated with an increase in penile diameter, see Fig. 3. When maximal penile diameter is reached, the arterial pulse either remains constant or decreases [11]. A photoelectric plethysmograph consists of a light source and a light detector. The optical absorption of blood is higher than the absorption of the surroundings. Therefore, the incoming light has a higher attenuation when the blood volume is higher [18].

Displacement sensor for axial length

For monitoring changes in penile length, a measurement of the displacement is favored. Resistive sensors contain an elastic material and senses a change in resistance due to changes in diameter and length [19]. Capacitive sensors monitor displacement by changes in distance between two parallel plates [20]. An advantage of resistive and capacitive sensors is their capability of measuring small displacements, and can therefore precisely monitor changes in penile length [19, 20]. For measuring changes in penile length, a stretchable sensor is necessary.

Strain gauges for radial rigidity and circumference

When simplified, the penis can be seen as a cylinder with two components: a blood reservoir (the corpora cavernosa) and the passive penile structures. During an erection, the outward pressure in the corpora cavernosa ($P_{\text{cavernosal}}$) and the inward pressure from the passive penile structures ($P_{\text{structures}}$) both increase, until the system is in equilibrium. An elastic band placed around the penis can be seen as an additional inward pressure (P_{elastic}). When the elastic band stretches (thus an increase in circumference), the inward pressure increases as well. This extra pressure means that the equilibrium (the penile circumference at which the sum of the forces is zero) at the location of the elastic band shifts. See equation 1. Note that this equation describes a local equilibrium shift, and does not involve the entire penile length.

$$P_{cavernosal}(t) = P_{structures}(t) + P_{elastic}(t). \quad (1)$$

An elastic band with a strain gauge around the penile shaft is able to monitor penile circumference. A strain gauge works as a piezoresistive sensor [21]. One individual band with a certain elasticity will not provide information about the rigidity of the underlying tissue. Therefore, minimal two elastic bands with a different stiffness and thus two equilibria are recommended. Since the material properties of the elastic bands are known, information about the underlying tissue can be acquired. The relation between the change in penile diameter and accompanying pressure by the elastic bands provides information about the rigidity of the penile tissue. To visualize the interplay between the properties of the penile tissue and the strain gauges, a schematic representation is given in Fig. 4. Note that the relations given in this figure are linear, while in reality these relations might have a linear part but are not completely linear.

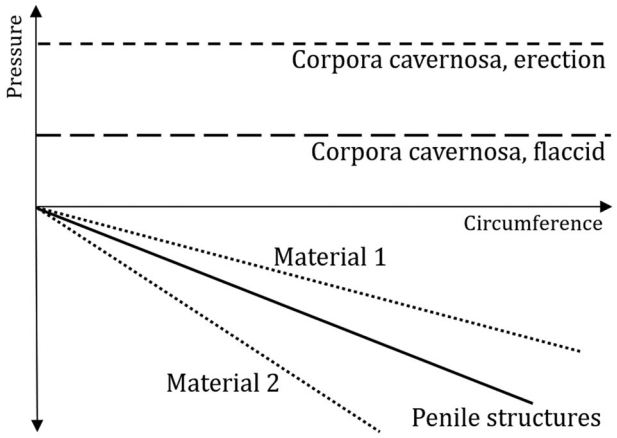

Fig. 4 Schematic representation of the corpora cavernosa (dashed lines) and passive penile structures (solid line) relative to the elastic bands (dotted lines). The stiffness (i.e., slope) of material 2 is bigger than the stiffness of material 1. During an erection, the outward pressure (upper dashed line) is higher compared to flaccid state (lower dashed line). The sum of the inward pressures created by the elastic band and the penile structures must be equal to the outward pressure created by the corpora cavernosa. During an erection, the pressure inside the corpora cavernosa increases and thus leads to an equilibrium-shift to the right on the x-axis.

Skin and cavernosal temperature sensors

Penile skin temperature has a bigger time constant than penile circumference, during both increases and decreases in sexual arousal [15]. For skin temperature, a thermocouple or thermistor are suitable options [22]. It is important that the influences of environmental thermal characteristics, heat conductivity and artifacts are taken into account. Increased skin temperature is a consequence of increased temperature in the erected corpora cavernosa. Therefore with adequate sensor depth settings also the temperature in the cavernosa should be measurable. The use of near-infrared (NIR) light can provide information about the temperature underneath the skin. Wearables are already being developed for infrared measurements [23]. This could be applied for penile tissue temperature measurements, especially in the corpora cavernosa.

Oxygenation sensor

Padmanabhan et al. studied the penile oxygen saturation in men with ED using a local tissue StO2 sensor and showed a significantly lower corporal penile StO2 in the flaccid penis. They made use of Optical Diffusion Imaging and Spectroscopy (ODIS) with the ODISsey Tissue Oximeter [24]. With the use of a tissue StO2 sensor with adequate depth settings, it should be possible to measure and visualize the saturation in the corpora cavernosa during flaccid state and during an erection.

Discussion

The current golden standard, the RigiScan, has several drawbacks. First of all, it causes physical discomfort and thereby disturbes natural sleeping patterns. Therefore, the results of the measured erections during REM sleep are less reliable. Other disadvantages are, for example, lack of updated software, lack of bluetooth compliance, the enormous size of a simple mechanical sensor and difficult instructions for both physician and patient. Due to the working mechanism of the RigiScan, it is not possible to miniaturize the current system. For all further sensor concepts described in this perspective, smaller dimensions are achievable. In general, a stretchable sensor is necessary to minimize the level of discomfort.

When choosing the most suitable sensor principle for this application, considerations will have to be made. First, a fundamental consideration is the information that can be derived from the nocturnal measurements. For example, a basic sensor may indicate whether there is an erection or not. However, when more detailed information about the duration and intensity of erection is required, a more complex sensor is necessary. For a wide range of uses, information about the duration and intensity of erections is favorable. With the available information, it is questionable whether the changes in temperature, arterial pulse and oxygen saturation can provide detailed information about the length and intensity of penile erections. Second, the data presentation should be taken into account as well. Urologists are familiar with the RigiScan and corresponding data presentation. Therefore, similar data presentation is favorable. The circumference and rigidity are physiological parameters with the same or a comparable data presentation, since these are the parameters measured by the RigiScan.

When looking at the penile anatomy, there are several layers between skin and the corpus cavernosa: skin, the superficial fascia, the deep fascia and the tunica albuginea [25]. When attaching a sensor to measure axial displacement during erection, the penile outer layers will move instead of the sensor itself. Because of movement of these layers relative to each other, it is impossible to attach a displacement sensor to a fixed point for axial length measurements. Moreover, these outer layers contribute to the tissue heat conductivity. The rate of increase and decrease of skin temperature depends on tissue conductivity and environmental temperature. Therefore, measuring the temperature inside the corpora cavernosa by a NIR temperature sensor provides more accurate information. However, little is known about the cavernosal temperature changes and its relation to the intensity and duration of an erection. Since these two components are important in the diagnostic process, cavernosal and penile skin temperature during erections should be studied thoroughly before it is put into practice.

Photoelectric plethysmography is suitable for peripheral vascular measurements and is sensitive to small amounts of pulsatile blood flow [18]. It is already being applied for continuous vascular monitoring in the evaluation of peripheral artery disease, for example in patients with atherosclerosis. The simplicity and low-cost of this method provide significant benefits to healthcare [26]. However, the changes in penile arterial pulse during tumescence and detumescence have not been studied in large populations. Nor is the exact location of the pulse sensor examined for application on the penis. Bancroft et al. [11]. found differences in the pattern of the penile pulse among 22 healthy subjects. In some subjects the penile pulse remained elevated during the full erection phase, while in others, the pulse amplitude lowered. Thus, further research on the changes in penile pulse during erection is needed.

Brow et al. described that cavernosal oxygen tension is lower in patients with arteriogenic and venogenic impotence compared to healthy individuals [17]. This might suggest that these patients have corporal fibrosis secondary to chronic ischemia [17]. Until today, little to nothing is known about oxygenation changes in cavernosal tissue during normal nocturnal erections. It is unknown whether physiologically normal nocturnal erections show a measurable decline in oxygenation of the corpora cavernosa during erection. A drawback of this method is the fact that it is unknown what time it takes for the erected penis before a decrease in cavernosal oxygenation occurs. Therefore, a graphic presentation of oxygenation will show a delay between the actual start of the nocturnal erection and the measurable erection.

Among the concepts discussed in this paper, an arterial pulse, temperature or oxygenation sensor would exert the least pressure and tensile forces. For monitoring circumference and rigidity, a certain radial pressure is necessary. The pressure applied to the penile skin should be sufficient to obtain valuable information about the physiological parameter, but should not disturb the natural sleep pattern. An overview of the different sensor principles and its advantages and disadvantages is given in Table 1.

Conclusion

New methods for measuring nocturnal erections are necessary. We discussed several sensor concepts as a successor for the still important, but outdated RigiScan. Axial length measurements seem impossible because of movement of the skin relative to the cavernosa. Skin and cavernosal temperature, penile arterial pulse, radial circumference and rigidity measurements, and saturation of the cavernosa are potentially feasible for home monitoring of nocturnal erections. Whether a combination of these techniques is favorable or only one of them should be studied more thoroughly.

Compliance with ethical standards

Conflict of interest The authors certify that they have no affiliations with or involvement in any organization with a financial interest in the outcome of the subject discussed in this manuscript. No financial assistance was received in support of this study.

References

1. Shamloul R, Ghanem H. Erectile dysfunction. Lancet. 2013;381: 153–65.
2. NIH Consensus Conference. Impotence. consensus development panel on impotence. J Am Med Assoc. 1993;270:83–90.
3. Elhanbly S, Elkholy A. Nocturnal penile erections: the role of rigiscan in the diagnosis of vascular erectile dysfunction. J Sex Med. 2012;9:3219–26.
4. Karacan I, William RL, Thornby JI, Salis PJ. Sleep-related penile tumescence as a function of age. Am J Psychiatry. 1975;132: 932–7.
5. Elhanbly SM, Abdel-gawad MM, Elkholy AA, State AF. Nocturnal penile erections: a retrospective study of the role of rigiscan in predicting the response to sildenafil in erectile dysfunction patients. J Adv Res. 2018;14:93–6.
6. Jannini EA, Granata AM, Hatzimouratidis K, Goldstein I. Controversies in sexual medicine: use and abuse of rigiscan in the diagnosis of erectile dysfunction. J Sex Med. 2009;6: 1820–9.
7. Bradley WE, Timm GW, Gallagher JM, Johnson BK. New method for continuous measurement of nocturnal penile tumescence and rigidity. Urology 1985;26:4–9.
8. Udelson D, Park K, Sadeghi-Najed H, Salimpour P, Krane RJ, Goldstein I. Axial penile buckling forces vs rigiscan™ radial rigidity as a function of intracavernosal pressure: why rigiscan does not predict functional erections in individual patients. Int J Impot Res. 2000;11:327–37.
9. Timm GW, Elayaperumal S, Hegrenes J. Biomechanical analysis of penile erections: penile buckling behaviour under axial loading and radial compression. BJU Int. 2008;102:76–84.
10. Borowitz E, Barnea O. Hemodynamic mechanisms of penile erection. IEEE Trans Biomed Eng. 2000;47:319–26.
11. Bancroft J, Bell C. Simultaneous recording of penile diameter and penile arterial pulse during laboratory-based erotic stimulation in normal subjects. J Psychosom Res. 1985;29:303–13.
12. Tal R, Mueller A, Mulhall JP. The correlation between intracavernosal pressure and cavernosal blood oxygenation. J Sex Med. 2009;6:2722–7.
13. Purohit RC, Beckett SD. Penile pressures and muscle activity associated with erection and ejaculation in the dog. Am J Physiol. 1976;231:1343–8.
14. Promodu K, Shanmughadas K, Bhat S, Nair K. Penile length and circumference: an Indian study. Int J Impot Res. 2007;19:558–63.
15. Kukkonen TM, Binik YM, Amsel R, Carrier S. Thermography as a physiological measure of sexual arousal in both men and women. J Sex Med. 2007;4:93–105.
16. Solnick RL, Birren JE. Age and male erectile responsiveness. Arch Sex Behav. 1977;6:1–9.
17. Brow SL, Seftel AD, Strohl KP, Herbener TE. Vasculogenic impotence and cavernosal oxygen tension. Int J Impot Res. 2000;12:19–22.
18. Challoner AVJ, Ramsay CA. A photoelectric plethysmograph for the measurement of cutaneous blood flow. Phy Med Biol. 1974; 19:317–28.
19. Weiss K, Worn H. The working principle of resistive tactile sensor cells. In: Proceedings of the IEEE International Conference on Mechatronics and Automation. 2005;471–6.
20. Zhu F, Spronck JW, Heerens WC. A simple capacitive displacement sensor. Sens Actuators A: Phys. 1991;26:265–9.
21. Chen X, Zheng X, Kim JK, Li X, Dong-Weon L. Investigation of graphene piezoresistors for use as strain gauge sensors. J Vacuum Sci Technol. 2011;29:29–34.
22. Matsukawa T, Ozaki M, Nishiyama T, Imamura M, Kumazawa T. Comparison of infrared thermometer with thermocouple for monitoring skin temperature. Crit Care Med. 2000;28:532–6.
23. Sahatiya P, Puttapati SK, Srikanth VVSS, Badhulika S. Graphene-based wearable temperature sensor and infrared photodetector on a flexible polyimide substrate. Flexible and Printed Electronics. 2016;1:025006.
24. Padmanabhan P, McCullough AR. Penile oxygen saturation in the flaccid and erect penis in men with and without erectile dysfunction. J Androl. 2007;28:223–8.
25. Hsu GL, Hsieh CH, Wen HS, Hsu WL, Wu CH, Fong TH, et al. Anatomy of the human penis: the relationship of the architecture between skeletal and smooth muscles. J Androl. 2013;25:426–31.
26. Alnaeb ME, Alobaid N, Seifalian AM, Mikhailidis DP, Hamilton G. Optical techniques in the assessment of peripheral arterial disease. Curr Vasc Pharmacol. 2007;5:53–9.

B Physiological parameters and constants

Table 8: *Overview of physiological parameters and constants.*

Parameter	**Symbol and unit**	**Condition**	**Value**
Circumference [48]	$[cm]$	flaccid erect	9.39 11.8
Penile length [48]	$L\ [cm]$	flaccid erect	9.19 14.3
Temperature	$T\ [K]$	blood skin*, flaccid skin*, erect	37 $°C$, 310 K [53] 31.9 $°C$, 305 K [15] 34.5 $°C$, 308 K [15]
Thermal conductivity [54]	$k\ [W/m/°C]$	blood connective tissue	0.52 0.39
Specific heat capacity [40]	$c_p\ [J/kgK]$	water at 290 K water at 305 K	4184 4178
Thickness of penile skin and fascias measured during curvature correction surgery	$[m]$	patient 1 patient 2 patient 3	0.0030 0.0020 0.0015
Thickness of tunica albuginea [36, 37]	$[m]$	flaccid	<0.002

* *In healthy subjects who are 18-29 years old [15].*

Table 9: *Input parameters for the heat transfer model. The length (L) represents the length of the penis. The inner radius (r_1) during flaccid condition is determined with the help of the thickness of the tunica albuginea according to literature, and the thickness of the penile skin and fascias. The latter is measured during penile curvature correction surgery (see Table 8). The inner radius (r_1) during erect condition is estimated with the help of the known outer radius (r_2) during an erection, and the value for r_1 during flaccid condition.*

Parameter	**Symbol**	**Value**
Flaccid condition		
Length	L	0.0919 m
Inner radius	r_1	0.0119 m
Outer radius	r_2	0.0149 m
Convective radius	r_{conv}	0.0349 m
Erection		
Length	L	0.143 m
Inner radius	r_1	0.0169 m
Outer radius	r_2	0.0188 m
Convective radius	r_{conv}	0.0388 m

C Specifications of the TM-220 Thermistor and TA-220 Control Module

"The TM-220 is a thermistor designed exclusively for biomedical applications in the range of 5 °C to 45 °C. Although low in cost, these highly stable, precision thermochips provide the reliability, tight interchangeable tolerances, geometries, and fast response times required. The resistance of the TM-220 changes depending on the temperature. The IX-TA-220 has a built-in circuit that measures the resistance of the sensor and LabScribe does a non-linear conversion to temperature. For better accuracy the TM-220 can be calibrated in software, using units conversion." - iWorx website [42]

Table 10: *TM-220 Thermistor specifications [42].*

Specifications	
Range	5 °C to 45 °C
Diameter of sensor	0.18 cm
Length of sensor	0.95 cm
Response time	15 seconds in still air, 2 seconds in still water.
Accuracy	0.5 °C

Table 11: *TA-220 Control Module specifications [55].*

A/D converter	
Sampling speed	200k Hz aggregate
Interface	USB 1.1, 2.0, full speed
General	
Power	12 VDC, 1.5 A
Enclosure dimensions	Plastic; 23 cm W, 15 cm D, 6.5 cm H
Weight	725 g
Software	LabScribe recording and analysis software

Table 12: *TM-220 Temperature vs Resistance [42].*

Temperature [°C]	**Resistance** [Ω]	**Temperature** [°C]	**Resistance** [Ω]	**Temperature** [°C]	**Resistance** [Ω]
0	32650.5	18	13679.8	36	6265.75
1	31032.1	19	13070.4	37	6016.47
2	29499.9	20	12491.6	38	5776.05
3	28052.4	21	11941.6	39	5546.53
4	26684.6	22	11418.9	40	5327.34
5	25391.2	23	10922	41	5117.97
6	24168.2	24	10449.5	42	4917.94
7	23011.2	25	10000	43	4726.77
8	21916.3	26	9572.32	44	4543.91
9	20879.8	27	9165.29	45	4369.33
10	19898.3	28	8777.79	46	4200.84
11	18968.6	29	8408.68	47	4040.81
12	18087.6	30	8057.31	48	3889.51
13	17252.6	31	7722.43	49	3743.17
14	16460.9	32	7403.29	50	3603.1
15	15710	33	7098.42		
16	14997.7	34	6808.36		
17	14321.6	35	6531.31		

D Additional graphs

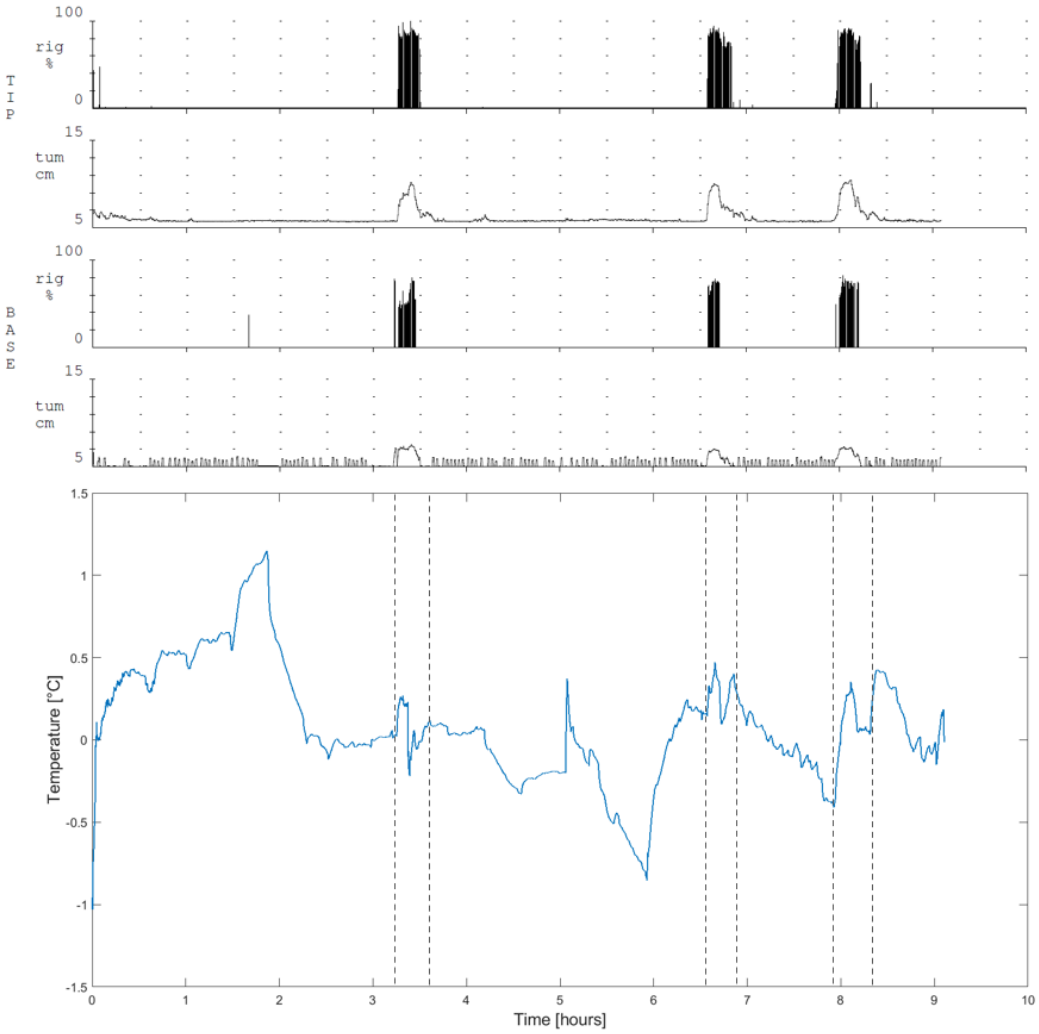

Figure 15: *An example of the output from a RigiScan measurement (four top graphs) and a thermistor measurement (bottom graph). The x-axes are equal. The output of the RigiScan consists of four graphs (from top to bottom): the rigidity measured by the TIP loop, the tumescence measured by the TIP loop, the rigidity measured by the BASE loop, and the tumescence measured by the BASE loop. During this measurement, the RigiScan monitored three erections which are visible by the peaks in the TIP and BASE graphs. The intervals that correspond with erections in the RigiScan data, were extracted in the temperature data, these are marked by the dashed lines.*

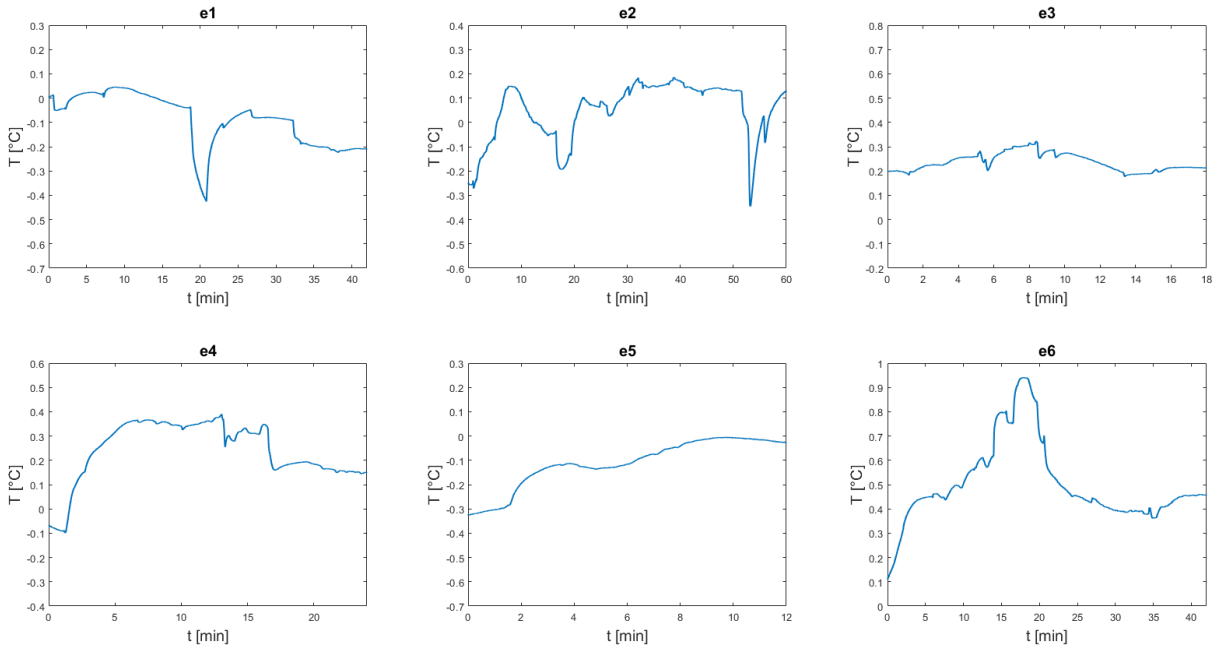

Figure 16: *Events 1, 2, 3, 4, 5 and 6. Y-axes are scaled equally.*

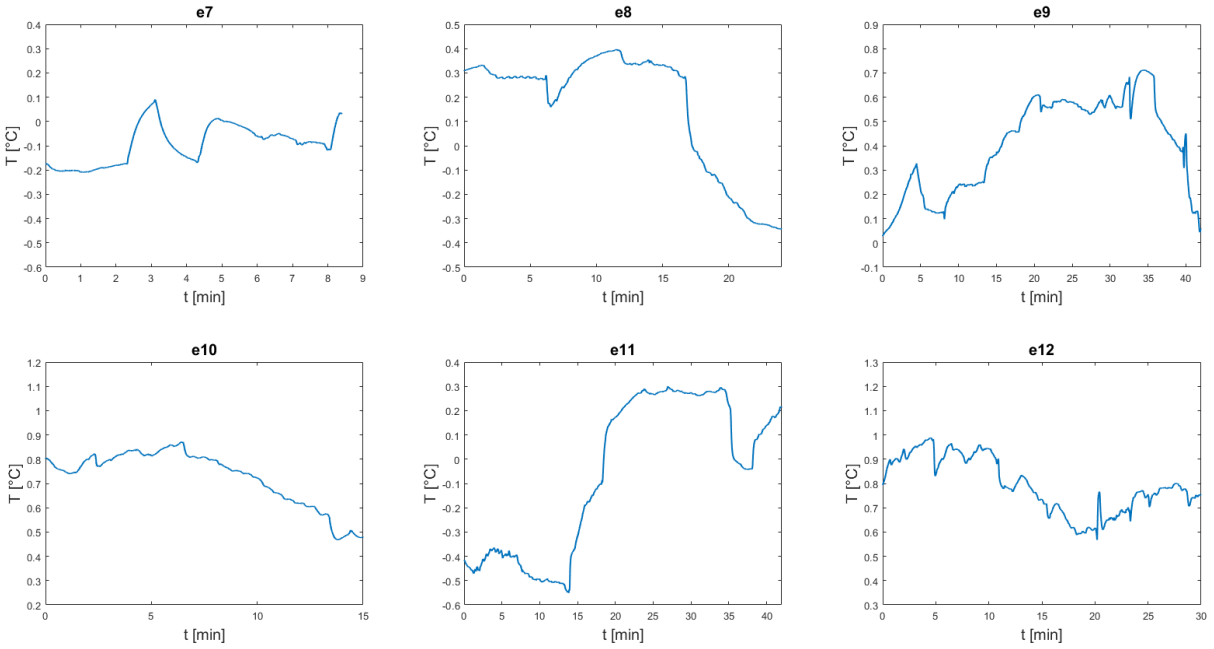

Figure 17: *Events 7, 8, 9, 10, 11 and 12. Y-axes are scaled equally.*

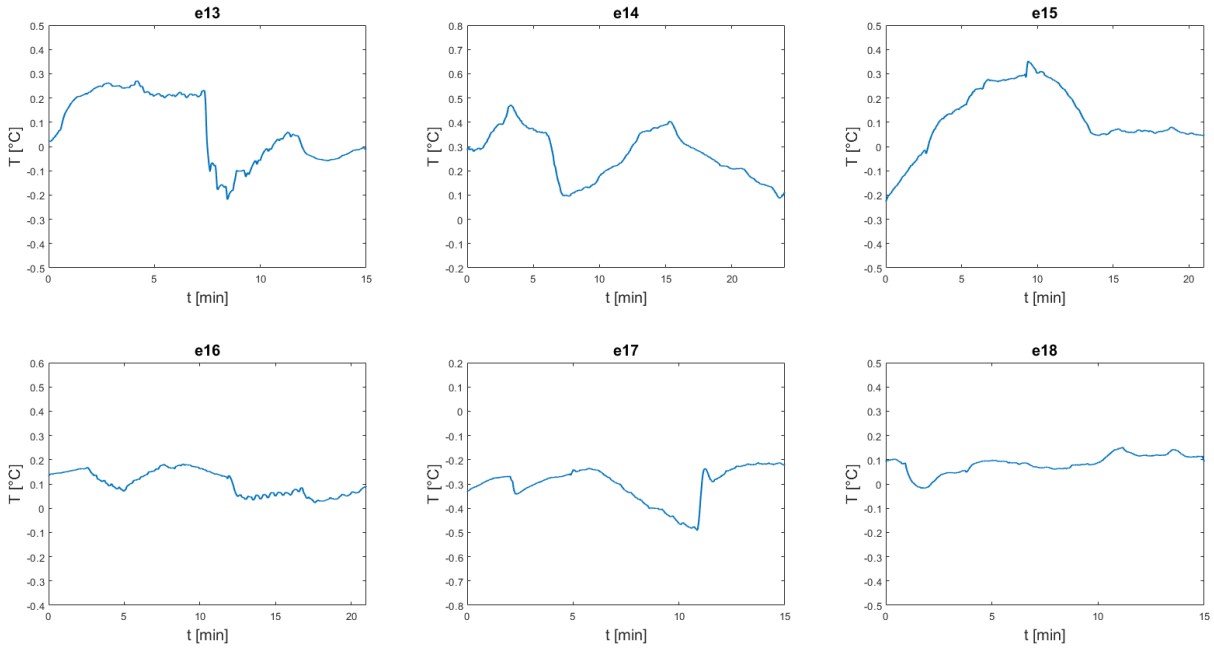

Figure 18: *Events 13, 14, 15, 16, 17 and 18. Y-axes are scaled equally.*

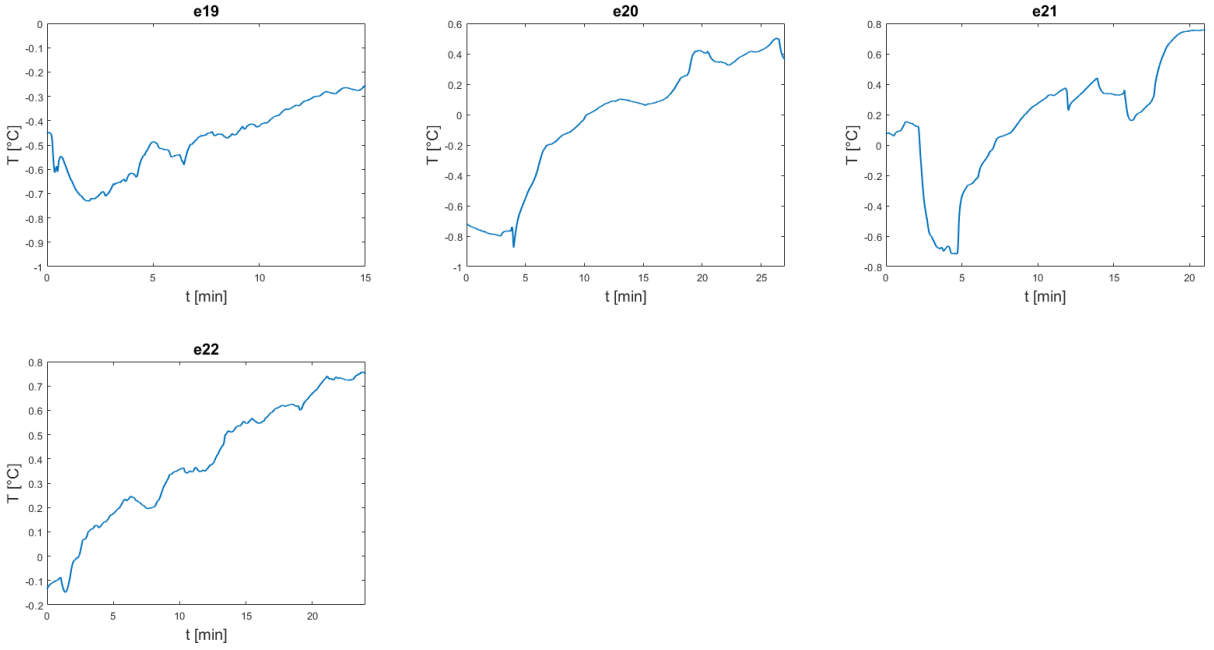

Figure 19: *Events 19, 20, 21 and 22. Y-axes are scaled equally, except for event 20 and 21.*

E FEELING HOT: measuring skin temperature for diagnosing erectile dysfunction - Summary

Thermistor for your mister: a research on measuring small skin temperature changes
Mathieu Broeders, Nina Hagen, Marit Kaptein, Michelle van der Neut
Technical Medicine Bachelor Thesis, University of Twente

A summary of the experimental part of the study

Introduction

The influence of clothing and blankets on small skin temperature differences is tested in an experimental setup, by four students. The aim of the experiment is to determine the effect of coverage on skin temperature changes of approximately 2 °C. The goal of the study is to translate the results from these experiments to penile skin temperature measurements in home setting.

Methods

During the experiment, the skin temperature of the dorsal hand was continuously monitored in different conditions. The dorsal side of the hand was chosen in this experiment, since there is little to no subcutaneous fat tissue and a smooth and flexible skin, just like the penile skin. Also, indirect cooling and heating of the skin temperature are possible in this body part.

Materials

The skin temperature was monitored with the TM-220 thermistor and accompanying TA-220 control module with LabScribe software from the iWorx Human Physiology kit (iWorx Systems inc, Dover, USA). Specifications of the thermistor and control module can be found in Appendix C. Infusion patches were used to attach the thermistor to the dorsal side of the hand. A glove (95% cotton, 5% elastane) and blanket (100% cotton) were used to simulate an increased environment temperature.

Study protocol

Changes in skin temperature of the dorsal side of the hand were obtained by heating and cooling of the fingertips. An increase in skin temperature of 2°C was achieved by putting the fingertips in warm water. Afterwards, a decrease of 2°C of the skin temperature was achieved by putting the fingertips in cold water. This process was repeated with bare skin, with a glove, and with a glove and blanket around the hand. These steps would imitate the penis without clothing (like the former studies in a laboratory setting) while wearing underwear, and while wearing underwear and laying in bed, respectively. The latter simulated the situation where the penile skin temperature is monitored remotely (at home) while a patient is asleep. An overview of this study protocol is given in Figure 20.

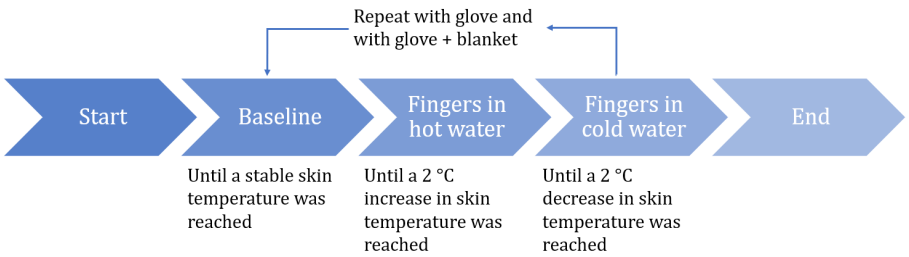

Figure 20: *Schematic overview of the study protocol. A stable skin temperature was defined as a temperature with a maximum deviation of 0.1 °C for at least 2 minutes.*

The experiments took place in the TechMed Centre at the University of Twente. The Ethics committee Natural Sciences and Engineering Sciences of the University of Twente assured ethical approval for the experiments. Measurements were conducted on four test subjects (age 20-22 years) several times. The main outcome parameter was the time it took to reach a $\Delta 2°C$ increase and decrease in skin temperature. The room temperature during the experiment was between 20 °C and 21 °C.

Data analysis
Data analyses were performed in Matlab R2018b and Microsoft Excel. Data were excluded from the study when the glove and the sensor became wet, or when no temperature rise of the skin was observed after putting the fingers in warm water. The median heating and cooling time in three groups were determined: the experiments with a bare hand, the experiments while wearing a glove, and the experiments with a glove and blanket. Statistical analyses were performed in SPSS version 26. Because of the non-normal distributed data a non-parametric test, the Friedman test, was applied. This test is based on ranks and can be used to test for differences between several related groups. If differences were found, the Wilcoxon signed-rank test was used to determine if significant differences existed when comparing two independent groups. Differences were stated significant if $|Z| > 1.96$ ($p < 0.05$) [56].

Results

The experiment was started 32 times, of which four experiments were cancelled since no increase in skin temperature was observed after putting the fingers in warm water. During one experiment the glove and sensor got wet, which was excluded as well. Furthermore, measurements where movement of the blankets might have influenced the skin temperature were also excluded. Eventually, there is data from 27 experiments with bare skin and while wearing a glove, and 25 experiments while wearing a glove and blanket. The median heating time increases when wearing a glove (median = 528 s) or a glove and blanket (median = 334 s), compared to the bare hand (median = 261 s). When it comes to the $\Delta 2°C$ decrease in skin temperature, the differences between the three groups are bigger; bare hand (median = 515 s), glove (median = 1288 s) and glove and blanket (median = 2674 s).

In Figures 21a and 21b, data from two experiments are shown. Figure 21a presents a complete temperature profile during the increase and decrease of $2°C$ in one test subject. Figure 21b depicts the temperature profile from the moment the fingers were put in cold water in one test subject. Note that the scales of the x-axes and y-axes differ.

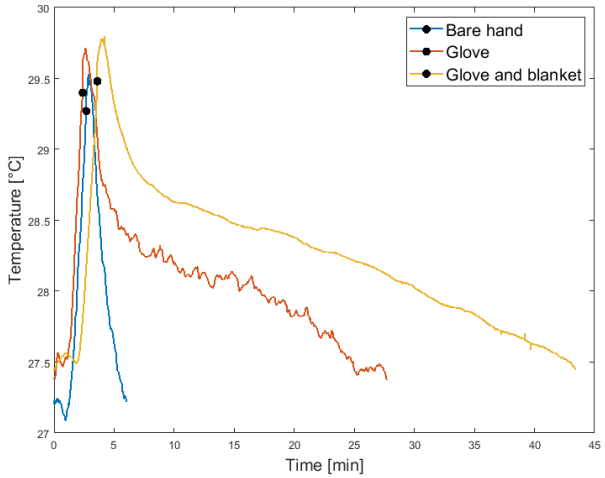

(a) *At t=0, fingers were put in hot water. At the black dots, the fingers were put into cold water.*

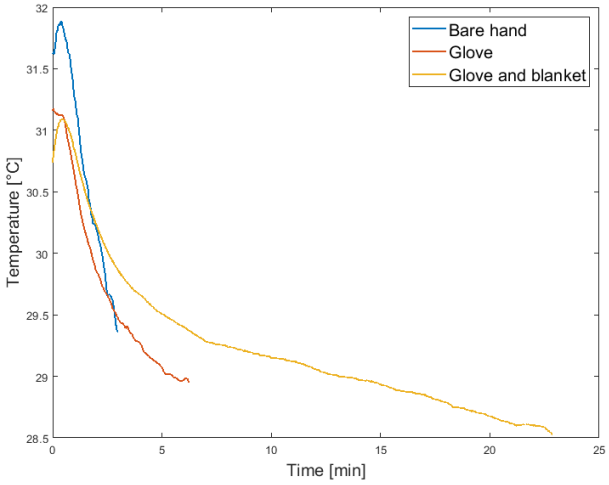

(b) *The decrease in skin temperature over time, after putting fingers in cold water at t=0.*

Figure 21: *Data from the experiments.* ***(a)*** *Provides an overview of the complete measurement, and* ***(b)*** *shows the temperature profile after the fingers were put in cold water. Note that the scale of the y-axes and x-axes is not equal.*

Statistical analyses were performed on the heating and cooling times of the skin. With the non-parametric Friedman test, differences between the groups were discovered, see Table 13. The non-parametric Wilcoxon signed-rank test reveals significant differences between the independent conditions, which can also be found in Table 13. During the increase of $2°C$, significant differences in the bare skin vs glove, and bare skin vs glove + blanket groups were found. When looking at the decrease of $2°C$, all comparisons between the independent conditions were found to be significantly different.

Table 13: *Statistics from the experimental study. Differences are considered significant if $|Z| > 1.96$ or $p < 0.05$.*

Friedman test	X^2	p
Increase of 2 °C	12.080	**0.002**
Decrease of 2 °C	42.091	< **0.001**
Wilcoxon signed-rank test	Z	p
Increase of 2 °C		
Bare skin vs glove	3.436	**0.001**
Bare skin vs glove + blanket	2.919	**0.004**
Glove vs glove + blanket	-1.170	0.242
Decrease of 2 °C		
Bare skin vs glove	4.445	< **0.001**
Bare skin vs glove + blanket	4.107	< **0.001**
Glove vs glove + blanket	4.107	< **0.001**

Discussion and conclusion

The time it takes to return to baseline temperature increases when wearing a glove or a glove and a blanket, compared to the bare skin. Due to clothing or a blanket, there exists a thin layer of heated air around the skin. This means that the temperature difference between the skin and the environment lowers, leading to a decrease in heat flow. Therefore, the skin cools down slower when wearing clothes or a blanket compared to the bare skin. Among the measurements, a great variety of heating and cooling times is seen. This might be explained by the varying baseline temperature.

The cooling time with clothes and blankets is relatively long compared to the cooling time of the bare hand in these experiments. However, the time between two nocturnal erections is still longer (an average of 85 minutes) than the cooling time in the experiments. Therefore, the distinction of separate erections through penile skin temperature monitoring should be possible.

When interpreting the results from the experiments, it should be kept in mind that the temperature of the water was not constant. During the experiments, the water temperature was intermittently corrected with warm or cold water. As a result, the water temperature fluctuated which may have influenced the skin temperature of the hand. Furthermore, during this experiment, there is focused on indirect heating of the skin by means of an external heat source (the warm water). However, the penile skin temperature increase occurs due to the accumulation of blood in the corpora cavernosa, which can be seen as an internal heat source. Also, the thermodynamic properties of the penile skin and the dorsal side of the hand may have similarities, but there are differences as well. Therefore, a direct translation of the results to clinical practice is not realistic.

In conclusion, the heating and cooling times of the skin covered by clothing or blankets significantly differ from the bare skin. According to these results, it should be possible to monitor nocturnal erections with an NTC thermistor at home.